050 KORTRAPPORT·BRIEF REPORT

Stephen R. Hudson, Herdis M. Gjelten, Ketil Isaksen and Jack Kohler

An assessment of MOSJ

Environmental status for atmospheric and terrestrial climate in Svalbard and Jan Mayen

MOSJ Miljøovervåking Svalbard og Jan Mayen

Kortrapport / Brief Report 050

MOSJ Miljøovervåking Svalbard og Jan Mayen

Stephen R. Hudson, Herdis M. Gjelten, Ketil Isaksen and Jack Kohler

An assessment of MOSJ

Environmental status for atmospheric and terrestrial climate in Svalbard and Jan Mayen

The Norwegian Polar Institute is Norway's central governmental institution for management-related research, mapping and environmental monitoring in the Arctic and the Antarctic. The Institute advises Norwegian authorities on matters concerning polar environmental management and is the official environmental management body for Norway's Antarctic territorial claims. The Institute is a Directorate within the Ministry of Climate and Environment.

Norsk Polarinstitutt er Norges hovedinstitusjon for kartlegging, miljøovervåking og forvaltningsrettet forskning i Arktis og Antarktis. Instituttet er faglig og strategisk rådgiver i miljøvernsaker i disse områdene og har forvaltningsmyndighet i norsk del av Antarktis. Instituttet er et direktorat under Klima- og miljødepartementet.

Addresses:

Stephen R. Hudson
stephen.hudson@npolar.no
Norwegian Polar Institute, Fram Centre
P.O Box 6606, Langnes
NO-9296 TROMSØ

Herdis M. Gjelten
herdis.m.gjelten@met.no
Norwegian Meteorological Institute
P.O Box 43, Blindern
NO-0313 OSLO

Ketil Isaksen
ketil.isaksen@met.no
Norwegian Meteorological Institute
P.O Box 43, Blindern
NO-0313 OSLO

Jack Kohler
jack.kohler@npolar.no
Norwegian Polar Institute, Fram Centre
P.O Box 6606, Langnes
NO-9296 TROMSØ

Norwegian Polar Institute, Fram Centre, NO-9296 Tromsø, www.npolar.no, *post@npolar.no*

Cover design:	Jan Roald, Norwegian Polar Institute (NPI)
Cover photo:	Sebastian Gerland, NPI. Zeppelin station, Svalbard
ISBN:	978-82-7666-423-2 (digital edition)
ISSN:	2464-1308 (digital edition)

Contents

Summary and evaluation

Significant warming has been observed across Svalbard over the last decades, and it is likely to continue, with natural variability on top of the anthropogenic warming signal. The warming has resulted in an increase in the fraction of precipitation that falls as rain and in the frequency of rain-on-snow events, which can lead to ice layers that make grazing more difficult. Total precipitation amounts are generally expected to increase, though the size of the increase is uncertain, as are current trends.

Greenhouse gas concentrations measured in Svalbard continue to increase, except for CFCs that were limited under the Montreal Protocol. These increases are broadly in line with global observations and trends, and will continue to force the climate toward a warmer state.

Longwave radiation emitted by the atmosphere to the surface has been increasing during the cold season since the 1990s, as a result of a warmer atmosphere with more greenhouse gases (including water vapour). Changes in cloud cover may also have affected the downwelling infrared radiation over this period. A somewhat smaller increase in cold season emission of infrared radiation from the surface was also observed over this period, directly related to the increase in surface temperature. The date in spring when the albedo first decreases below a threshold indicating snowmelt has shifted earlier, with a trend of about five days per decade.

Ground temperatures in the permafrost are increasing at all depths down to 80 m, indicating multi-decadal warming. The increase in the upper 10–20 m is substantial, and the active layer thickness, with summer thawing, has been increasing over recent decades. Some permafrost in low-lying areas of bedrock is expected to thaw completely by the end of the century, but most areas will remain perennially frozen at depth. Increasing the temperature and active layer thickness of permafrost can drive a climate feedback through the release of carbon stored in the permafrost, in the form of methane (CH_4) and carbon dioxide (CO_2), both of which are greenhouse gases.

Overall, glaciers in Svalbard are losing more ice through melting and calving than they are accumulating through snowfall. All of the well observed glaciers are shrinking, and satellite measurements confirm that the archipelago as a whole is losing mass. This loss of glacier mass and area is changing the landscape and contributing to sea-level rise. Variability in the mass balance in Svalbard is primarily driven by summertime melt variations. Lengthening of the melt season and warmer summers in coming decades are likely to continue driving increased glacier melting.

While there are extensive data records from Ny-Ålesund, Longyearbyen, Barentsburg and Hornsund, and long meteorological records from Bjørnøya, Jan Mayen and Hopen, most of the archipelago is not well observed, especially the eastern half of Spitsbergen and all of Nordaustlandet. There are significant climate gradients across the archipelago, so it is important to try to observe the undersampled areas as well as possible. There are field campaigns and new automatic weather stations that may help to fill in these gaps and provide an understanding of the spatial variability. Satellite observations also provide an opportunity to fill in these gaps, though the small scale topographical variability of many parts of Svalbard can make the interpretation of satellite data

challenging if the resolution is not better than about a kilometre. Higher resolution satellite observations and better techniques for interpreting them could also help to fill the gaps.

The changes described in this report are much more strongly driven by global activities than local ones. Regulations in Svalbard, such as the ban on ships burning heavy fuel oil and the restrictions on snowmobile traffic to much of the islands, help to mitigate local effects of human activities. However most of the change is driven by global climate changes caused by emissions of greenhouse gases globally. Norway is taking action, together with most nations, to address this problem, but it will take time and global efforts to slow these changes. Norway's environmental goals related to climate are sound, but implemented by Norway alone, they will not have a large effect. Adequate monitoring of the changes occurring in Svalbard is important for evaluating whether the goals need to be updated, especially in light of the enhancement of warming that has been observed there, relative to the global mean.

Oppsummering på norsk (Norwegian summary)

Det er observert en vesentlig oppvarming av Svalbard de siste tiårene. Den menneskeskapte oppvarmingen kommer i tillegg til naturlige variasjoner, og er forventet å fortsette framover. Oppvarmingen har ført til økning i andelen av nedbør som faller som regn og i antall tilfeller av regn-på-snø, noe som kan føre til dannelse av islag som gjør beiting vanskeligere. Den totale nedbørsmengden forventes å øke, men det er usikkerhet knyttet til størrelsen på økningen og trendene for de siste tiårene.

Konsentrasjonen av drivhusgasser som måles på Svalbard fortsetter å øke, bortsett fra KFK-gasser. Disse endringene er stort sett i tråd med globale observasjoner og trender, og fører til at temperaturen vil fortsette å stige.

Langbølget (infrarød) stråling fra atmosfæren til jordoverflaten om vinteren har økt siden 1990-tallet, som følge av en varmere atmosfære. Endringer i skydekket kan også ha påvirket den infrarøde innstrålingen over denne perioden. En mindre økning av infrarød utstråling ble også observert i vintersesongen i denne perioden. Dette er direkte knyttet til økningen i overflatetemperaturen. Tidspunktet på våren når albedoen faller under en viss terskel som indikerer at snøen har smeltet, kommer tidligere og tidligere, med en trend på ca. fem dager per tiår.

Jordtemperaturen i permafrosten øker i alle dybder ned til 80 m. Det indikerer en oppvarming som har pågått over flere tiår. Temperaturøkningen i de øvre 10–20 m er betydelig, og tykkelsen av det aktive laget som tiner om sommeren har økt de siste tiårene. Noe permafrost i lavtliggende fjellområder forventes å tine helt mot slutten av dette århundret, men de fleste områdene på Svalbard vil fortsatt ha permafrost. Økningen i jordtemperatur og dybden av det aktive laget, kan føre til utslipp av drivhusgassene karbondioksid (CO_2) og metan (CH_4) som nå er lagret i de frosne jordmassene.

Samlet mister isbreer på Svalbard mer is gjennom smelting og kalving enn hva de får tilført fra nytt snødekke. Alle isbreene der det pågår systematiske målinger krymper, og satellittmålingene viser at

breer over hele Svalbard mister masse. Dette tapet av masse og areal endrer landskapet og bidrar til havnivåstigning. Forskjellene i bresmeltningen er primært drevet av smeltevariasjoner om sommeren. Forlengelse av smeltesesongen og varmere somre i de kommende tiårene vil trolig fortsette å føre til økt bresmelting.

Det eksisterer et stort antall meteorologiske dataserier fra Ny-Ålesund, Longyearbyen, Barentsburg og Hornsund, og lange tidsserier fra Bjørnøya, Jan Mayen og Hopen. Derimot er det få observasjoner fra resten av øygruppa, og særlig gjelder det den østlige delen av Spitsbergen og hele Nordaustlandet. Det er betydelige klimagradienter på tvers av Svalbard. Derfor er det viktig å få så god datadekning som mulig også i disse områdene. Det drives per i dag feltarbeid, og det er i ferd med å bli etablert nye automatiske værstasjoner som vil bidra til å fylle disse kunnskapshullene. Dette vil gi økt forståelse av den romlig variabiliteten i klimaet på Svalbard. Satellittobservasjoner gir også mulighet til å fylle disse hullene. Men tolkning av satellittdata kan være utfordrende fordi oppløsningen per i dag ikke er bedre enn én kilometer samtidig som den geografiske variabiliteten på Svalbard gjerne har en finere skala. Satellittobservasjoner med høyere oppløsning, og bedre teknikker for å tolke dem, kan også bidra til å fylle kunnskapshullene.

Endringene som er beskrevet i denne rapporten er først og fremst drevet av globale utslipp av klimagasser. Forskrifter for Svalbard, som gjelder forbud mot tungolje som drivstoff i skip, og restriksjonene på snøscootertrafikk, bidrar til å redusere lokale effekter av menneskelig aktivitet. Norske myndigheter bidrar i et bredt internasjonalt samarbeid med å begrense utslipp av klimagasser, men det vil ta tid å bremse klimaendringen og dens effekter på Svalbard. God overvåkning av klimaendringene og effektene på Svalbard er nødvendig for å evaluere de nasjonale miljømålene i tiden fremover. Dette er særlig viktig siden klimaendringene i norsk del av Arktis er langt større enn det globale gjennomsnittet.

Kronebreen. Photo: K. Lindbäck, Norwegian Polar Institute, 2015.

1. Introduction

The Arctic has experienced greater warming than most of the planet in recent decades, and Svalbard and the surrounding seas are among the most rapidly changing parts of the Arctic (Overland, et al. 2017). These changes are initially driven, in large part, by increases in greenhouse gas concentrations due to human activities (IPCC 2013). However, they are enhanced in the region by a variety of feedbacks that amplify warming in the Arctic (Overland, et al. 2017). Svalbard's climate is also influenced by variations in the temperature of the West Spitsbergen Current, which carries relatively warm Atlantic water into the Arctic and limits sea-ice formation to the west and north of Svalbard. The water in this current has been warmer recently than in the past decades and centuries (Spielhagen, et al. 2011), which has led to less sea ice in the region (Onarheim, et al. 2014), bringing a more maritime climate to parts of Svalbard.

Warming in the region has many impacts on other aspects of the climate, ecosystems, glaciers and infrastructure. Precipitation amounts are changing, and the fraction of precipitation falling as rain rather than snow is increasing, also in winter. Wintertime rain events create ice layers that hinder grazing by reindeer, and the loss of sea ice drives ice-dependent seals away, in turn affecting polar bears. Glaciers in Svalbard are losing mass as summertime melt increases, which in turn contributes to sea-level rise and increased areas of exposed rock and tundra. Thickening the active layer in permafrost (the top layer that thaws in summer) increases the risk of landslides and of damage to roads and buildings built on the permafrost. These represent just a selection of the impacts of Svalbard's changing climate.

This report presents an update of some of the terrestrial climate-related drivers and indicators of and responses to the ongoing climate change observed in Svalbard. It begins by looking at changes in greenhouse gas concentrations, which are the primary driver of the changes. Next it presents trends and observations in solar and emitted infrared radiation (light), which largely determine the surface temperature, and which are affected by greenhouse gas concentrations (infrared light) and by changes in the surface conditions (solar absorption). Trends and observations of temperature and precipitation, which are affected by the radiation, are then examined, followed by the resulting impact on snow cover, permafrost and the mass balance of Svalbard's glaciers.

Most of Svalbard is uninhabited and difficult to reach, so there is a limited amount of observations from the region. This results in the report being biased toward the observation sites, especially Ny-Ålesund in northwest Spitsbergen, where many institutions carry out a large suite of observations. Longyearbyen, also in western Spitsbergen, has many observations, along with the meteorological stations in Hornsund and Barentsburg and on the islands Hopen, Bjørnøya (Bear Island) and Jan Mayen. Models and satellite data help to fill some of the gaps, along with results from remote field work.

2. Greenhouse gases

The atmospheric concentration of 24 greenhouse gases is measured at the Zeppelin Observatory in Ny-Ålesund, among these are the most important greenhouse gases such as CO_2, CH_4, N_2O and F-gases (CFCs, HCFCs, HFCs and SF_6). These are gases that contribute to the global warming of the climate system and whose concentration is affected by human activity. Observations of CO_2 started in 1988. Observations of CH_4 and F-gases started in 2001, while observations of N_2O started in 2009. The location is minimally influenced by local sources of climate gases and is therefore an ideal site for monitoring the global, long-term development in greenhouse gas concentration in the atmosphere. The Arctic location is also important because the Arctic is a particularly vulnerable region.

The Zeppelin Observatory in Ny-Ålesund. Photo: H. T. Markussen, Norwegian Polar Institute, 2018.

2.1 Carbon dioxide (CO_2)

Carbon dioxide is the single most important contributor to the radiative forcing by long-lived greenhouse gases, accounting for about 65% of the total forcing by these gases. The CO_2 concentration in the atmosphere has increased to 145% of the value in pre-industrial times, and the concentration today is the highest in at least 800 000 years (WMO 2017). The increase is mainly due to human activity, such as combustion of fossil fuels and land-use change (mainly tropical deforestation) (WMO 2017).

The atmospheric daily mean concentration of CO_2 at the Zeppelin Observatory is shown in Figure 1. The figure clearly depicts an increase in the concentration since the beginning of the observations, in 1988. The years 2015 and 2016 were the first with annual mean concentrations above 400 parts per million by volume (ppm), though wintertime values have been above that threshold for most of the current decade (Myhre, et al. 2015; 2017). In addition to seasonal variations, there are also episodes with higher levels due to transport of pollution from various regions, generally from central Europe or Russia (Myhre, et al. 2015). The linear trend in the annual mean concentration at Zeppelin

Observatory over the period 2001–2016 is 2.5 ppm/year, slightly greater than the global mean growth rate for the past decade (WMO 2017; Myhre, et al. 2017).

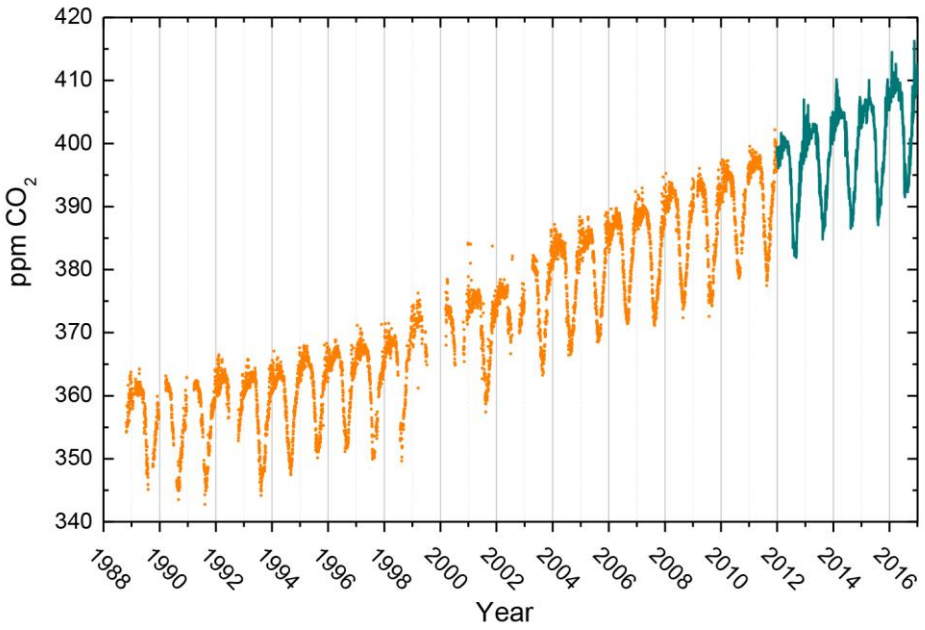

Figure 1: The atmospheric daily mean CO_2 concentration measured at Zeppelin Observatory for the period mid-1988–2016. Prior to 2012, the measurements were performed by ITM University of Stockholm (orange dots). NILU started their measurements in 2012 (green line). Pre-industrial concentrations of CO_2 were around 280 ppm (WMO 2017). Figure from Myhre, et al. (2017).

2.2 Methane (CH_4)

Methane is the second most important contributor to the radiative forcing by long-lived greenhouse gases, with a contribution of 17%. The atmospheric concentration of CH_4 has increased to 257% of its pre-industrial concentration. The main sources are ruminants, rice agriculture, landfills, fossil fuel exploitation (especially natural gas), biomass burning, termites and boreal and tropical wetlands. About 60% of the emissions are anthropogenic (WMO 2017).

The atmospheric daily mean concentration of CH_4 at the Zeppelin Observatory is shown in Figure 2. The figure depicts an increase in CH_4 concentration since 2001, but the increase is not as steady as for CO_2. There were some higher concentrations in the period 2008–2010 then a couple of years with lower concentrations before higher concentrations again in recent years.

Myhre, et al. (2017) show that the annual mean concentration at Zeppelin Observatory in 2016 was 1932 parts per billion by volume (ppb). One of the highest CH_4 concentrations at Zeppelin was observed 15 February 2014, and this was due to transportation of Russian industrial pollution (Myhre, et al. 2015). The transportation pattern for this incident is also shown in Figure 2. Over the period 2001–2016, the linear trend in the annual mean concentration at Zeppelin is 5.6 ppb/year, which is slightly less than the global mean growth rate over the past decade, 6.8 ppb/year (Myhre, et al. 2017; WMO 2017).

Currently, the observed increase over the last years is not yet explained or understood. It is essential to investigate whether the increase since around 2005 is caused by emissions from large point sources or by newly initiated processes releasing CH_4 to the atmosphere, e.g. thawing permafrost (Myhre, et al. 2017; WMO 2017).

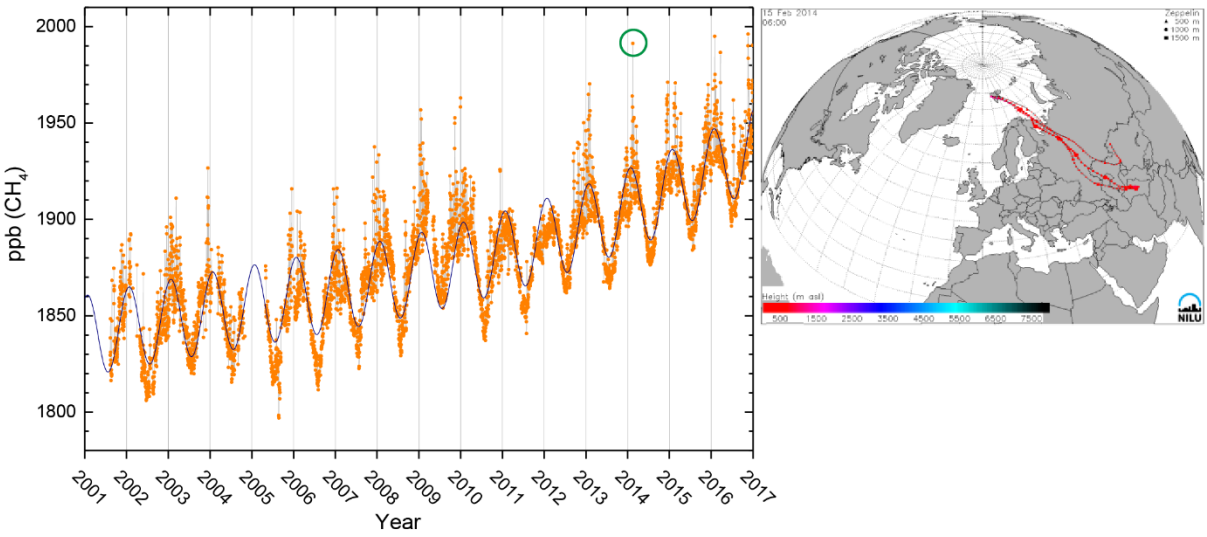

Figure 2: Observations of daily averaged methane mixing ratio for the period 2001–2016 at the Zeppelin Observatory are plotted on the left as orange dots. The black line shows an empirically modelled background methane mixing ratio. The right panel shows the transport of air to Zeppelin on 15 February 2014, when a maximum CH_4 concentration was observed (marked with green circle in left panel). Figure after Myhre, et al. (2015; 2017).

2.3 Nitrous oxide (N_2O)

Nitrous oxide is the third most important contributor to the radiative forcing by long-lived greenhouse gases. Its contribution is 6%, and the atmospheric concentration of N_2O has increased to 122% of its pre-industrial value. The main sources are oceans, soil, biomass burning, cultivated soil, fertilizer use and various industrial processes. About 40% of the sources are anthropogenic (WMO 2017).

The atmospheric daily mean concentration of N_2O at the Zeppelin Observatory is shown in Figure 3. The 2016 annual mean concentration was 329 ppb, very close to the global mean value. The observation series is too short for trend analysis, but it shows an increase of about 1 ppb in the annual mean concentration each year from 2011 to 2016, which is slightly larger than the global mean growth rate over the past decade (0.9 ppb/year) (Myhre, et al. 2017; WMO 2017).

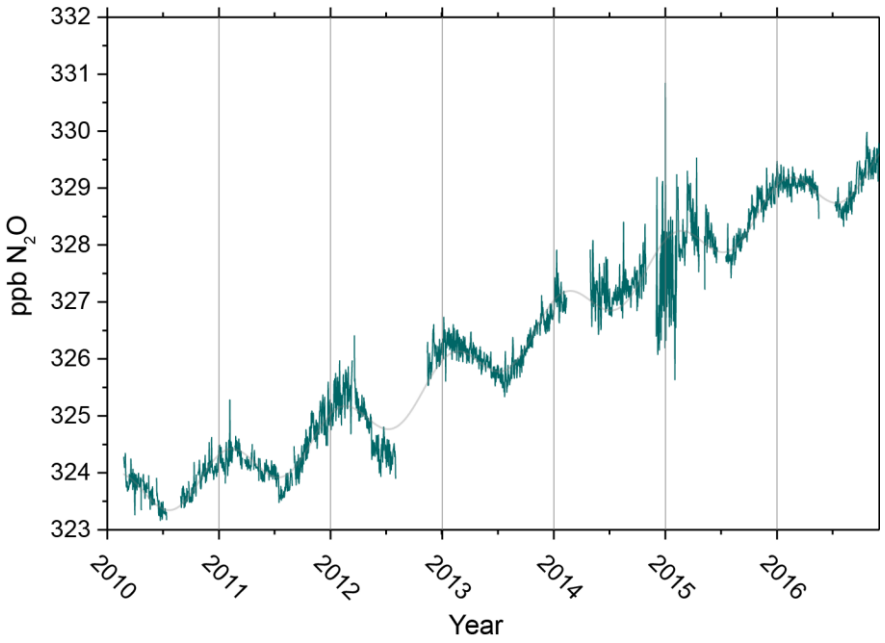

Figure 3: Measurements of N_2O at the Zeppelin Observatory for 2010–2016. The grey line is an empirically modelled N_2O mixing ratio. The high variability in 2014/2015 is due to instrumental problems. Figure from Myhre, et al. (2017).

2.4 Other greenhouse gases

CFCs, HCFCs, HFCs and SF_6 are greenhouse gases with purely anthropogenic sources. These gases have high global warming potential. Many of them have long atmospheric lifetimes, so although the atmospheric concentration of these gases is very low, they contribute about 12% to radiative forcing by long-lived greenhouse gases (Myhre, et al. 2017; WMO 2017).

Globally, CFCs are decreasing in response to the limitations placed on their use by the Montreal Protocol. These gases have a strong ozone depleting effect, in addition to high global warming potential. The CFCs measured at Zeppelin Observatory are now decreasing or at least stabilized. Most of their replacement gases (HCFCs and HFCs) and SF_6 continue to increase significantly in concentration at Zeppelin Observatory (Myhre, et al. 2017).

3. Atmospheric radiation

As the radiation components drive much of the heating and cooling of the surface, monitoring them is important to understanding and observing changes to the climate system. In Svalbard, such monitoring has been ongoing at Ny-Ålesund since 1981.

Ørbæk et al. (1999) examined seasonal variations in the radiation components at Ny-Ålesund in the 1980s and 1990s. They also used satellite observations to gain a broad picture of the spatial variability of these variations around Svalbard and the surrounding ocean. They highlighted some characteristics of the seasonal variation in the radiation components in Ny-Ålesund.

These included a peak in incoming solar radiation around the start of June, rather than at the June solstice. While this offset could be related to a seasonal change in cloud properties, Ørbæk et al. attributed it to the decrease in surface reflectance (albedo) as the snow melted in June, which reduced multiple scattering between the surface and sky. This reduction in multiple scattering reduced the downwelling sunlight more than the small increase in insolation during those weeks could offset. Another characteristic they described was a relatively constant mean value of incoming infrared radiation emitted by the atmosphere during the winter half of the year, but with large day-to-day variability. This variability reflected the swing from clear, cold conditions, with low infrared fluxes, to cloudy, warmer conditions, with high infrared fluxes, which is typical of the two-state Arctic winter (Graham, et al. 2017b).

More recently, Maturilli, et al. (2015) examined the variations and trends in the radiation components and albedo over the period 1993–2013, providing the opportunity to look at ongoing trends and changes from the earlier period to the recent period.

3.1 Solar radiation

There have been no significant changes to the amount of solar radiation arriving at the top of the Earth's atmosphere over the last 50 years (IPCC 2013), so any changes in solar radiation reaching the surface would be tied to other changes. One possible cause is change in cloud cover or particles in the atmosphere, which both scatter and absorb the light on its way to the surface. Another possibility is changes in surface reflectance, which affects the amount of downwelling solar radiation by changing the amount of light that is reflected by the surface and re-scattered back to the surface by the atmosphere.

Over the 1993–2013 period, Maturilli, et al. (2015) reported a decrease in incoming solar radiation in spring of 6 W m^{-2}/decade, which was not statistically significant given the inter-annual variability, shown in Figure 4. For summer, they reported an even less significant increase of 5 W m^{-2}/decade. Average values in spring and summer are about 125 and 175 W m^{-2}, respectively. A springtime decrease could result from reduced surface albedo, due to either earlier snowmelt in May or reduced sea ice in the nearby fjord, that results in less multiple scattering (Grenfell and Perovich 2008). It could also indicate an increase in cloudiness or cloud thickness. The summer increase, if meaningful, would likely indicate a decrease in cloud cover or cloud thickness.

Figure 4 also shows changes in seasonally averaged reflected solar radiation in Ny-Ålesund. A negative trend is seen in both spring (10 W m^{-2}/decade) and summer (7 W m^{-2}/decade); Maturilli et al. ascribe a degree of statistical significance to the spring trend, but not to the summer trend. The decrease in reflected solar radiation in summer, when incoming solar radiation was increasing, must be due to a decrease in the surface albedo, most likely caused by reduced snow cover in June, though changes to the underlying tundra could also play a role. The decrease in spring is partly tied to the decrease in incoming sunlight in spring, but since it is larger than the decrease in incoming sunlight, it also indicates a decrease in albedo in spring, when changes to the snow cover are the most likely driving factor. Those changes could be earlier removal of the snow, but other changes such as a thinner snow cover or warmer snow with larger grains would also reduce the albedo.

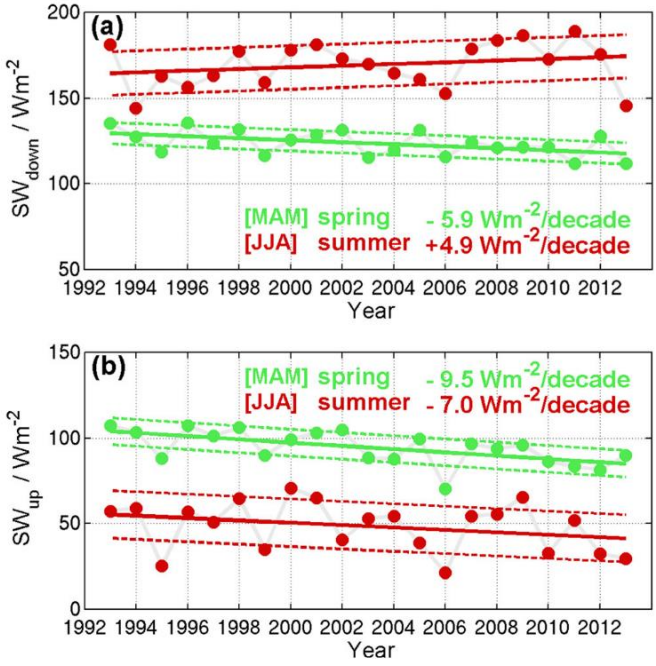

Figure 4: Average (a) incoming and (b) outgoing solar radiation flux in Ny-Ålesund in spring and summer for each year from 1993 to 2013, along with the resulting trends. Figure from Maturilli, et al. (2015).

3.2 Albedo

The very high albedo of snow (>0.75) compared to that of bare tundra, rock or open water (<0.25) means that there are large seasonal changes in the fraction of incoming sunlight that is absorbed by the surface. Figure 5 shows this seasonal variation through each year from 1993 to 2013. It shows that, in most years, the springtime decrease associated with snow melt occurs over a period of days. This decrease in albedo results in more than a four-fold increase in absorbed sunlight (from about 20% to more than 80% of incoming), dramatically increasing surface heating and evaporation by the incoming sunlight.

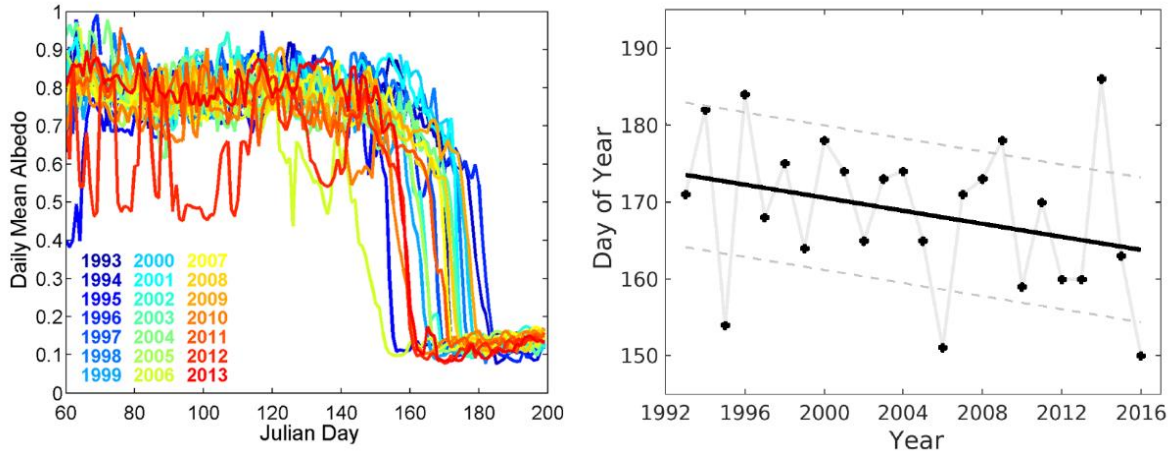

Figure 5: The progression of daily-mean albedo in Ny-Ålesund from 1 March to 19 July each year from 1993 to 2013 (left), and the first day each year with a daily-mean albedo less than 0.2 (right), a proxy for complete snow melt under the radiation sensors; days 152 and 182 correspond to 1 June and 1 July, respectively, in non-leap years. The plot on the left is from Maturilli, et al. (2015), and that on the right is updated from the same (M. Maturilli, personal communication).

Another reason the timing of the snow melt is important is that the removal of the snow cover allows the surface to warm above the freezing point, to which it is limited while snow remains. The right panel in Figure 5 shows that this transition has been happening earlier, on average, than in the past. The date on which the albedo first drops below 0.2 (a proxy for complete snow melt at the radiation site) is becoming earlier by about five days/decade. Ørbæk, et al. (1999) showed that the average albedo for the period 1981–1997 dropped below 0.2 on day 180, in line with the early part of the period presented by (Maturilli, et al. 2015). While the onset of melt decreases the snow albedo by 0.1–0.2, it is the complete melt off of snow that drastically darkens the surface, so an increase in late spring snow thickness could counteract an earlier melt onset, as discussed in the section on snow cover.

3.3 Emitted infrared radiation

One of the most striking trends reported by Maturilli, et al. (2015) was an increase of 16 W m^{-2}/decade in infrared light from the atmosphere to the surface in winter, as shown in Figure 6. For summer, they report only a small decrease (1 W m^{-2}/decade). Some of the wintertime increase is tied to the strong warming they report in winter, but it is likely that a change in cloud cover, i.e. increased cloud occurrence, thickness or temperature, or an increase in water vapour also contributed to the change. The average flux of infrared light from the atmosphere during the period 1981–1997 was similar to the early values reported by Maturilli, et al. (Ørbæk, et al. 1999). Any decrease in summertime emission from the atmosphere is likely tied to decreased emission from clouds or water vapour, since there was also some observed warming near the surface in summer and no reports of cooling in the remainder of the lower atmosphere (troposphere).

Figure 6 also shows trends in infrared light emitted by the surface in summer and winter. These are strongly tied to changes in the surface temperature in Ny-Ålesund, as the emitted infrared energy is almost entirely determined by the surface temperature. There is an observed increase in both seasons, though that in summer, 2 W m^{-2}/decade, is much smaller than that in winter, 12 W m^{-2}/decade. The reported trends in near-surface air temperature, 3.1 °C/decade in winter and 0.7 °C/decade in summer (Maturilli, et al. 2015), would drive an increase in emitted infrared flux of about 13 and 3 W m^{-2}/decade, respectively.

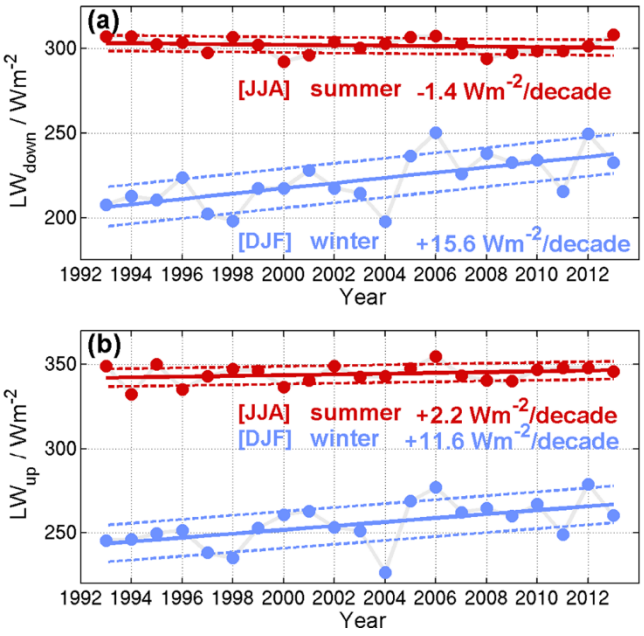

Figure 6: Average (a) incoming and (b) outgoing thermal infrared radiation flux in Ny-Ålesund in spring and summer for each year from 1993 to 2013, along with the resulting trends. Figure from Maturilli, et al. (2015).

3.4 Ultraviolet radiation

Ultraviolet radiation is part of the solar radiation spectrum, at the shortest wavelengths that penetrate the Earth's atmosphere. In this sense it is a component of the section above; however, light at these wavelengths not only warms the surface, but also has negative impacts on cells that are exposed to it. For this reason, and because human-induced changes in the ozone layer can influence the amount of ultraviolet light that penetrates the atmosphere, it is also measured separately in Ny-Ålesund.

During the period 1979–1997 there was significant loss of ozone over Svalbard, especially in springtime. Since then, ozone levels have stabilized at about 2% below pre-1980 levels; however, significant negative anomalies still occur, such as in February 2016, when the average ozone level over Ny-Ålesund was 27% below the long-term mean for the month (Svendby, et al. 2017).

Observations of ultraviolet radiation in Ny-Ålesund made since 1996 show a small but statistically insignificant negative trend (Svendby, et al. 2017). This result is in line with the stable levels of ozone over the region during this period. Day-to-day and seasonal variability are much more significant, especially due to changes in cloud and snow cover.

3.5 Black carbon

Black carbon aerosol (BC; essentially airborne soot) is a very effective absorber of solar radiation. While airborne, BC warms the atmosphere directly when it absorbs sunlight, and it also affects cloud formation processes (Gogoi, et al. 2016). When BC is deposited in the snowpack, either by falling with the snow (wet deposition) or falling on the top of the snowpack (dry deposition), it can reduce the snow's albedo, potentially leading to surface warming or melting earlier in spring than would be the case for clean snow (Forsström, et al. 2013).

BC is emitted through natural wildfires and human burning of fossil fuels, waste, biomass, etc. Once emitted, BC can be transported long distances in the atmosphere before falling out. Atmospheric concentrations of BC over Ny-Ålesund are generally higher in the winter and spring (Gogoi, et al. 2016; Sinha, et al. 2018) than in summer and autumn. Sinha, et al. (2018) also show a peak in BC concentration in falling snow in January–March. The exact relationship between BC in the atmosphere and BC in snow is complicated by a variety deposition processes that are still being studied. Forsström, et al. (2013) present measurements of the concentration of BC in snow from many sites around Svalbard; generally the concentrations in Svalbard are similar to other remote Arctic locations and to remote areas in Scandinavia, but generally less than one quarter the concentrations found in snow near towns in Scandinavia. The concentrations reported in Svalbard are at the lower limit of what is needed to detectably lower the snow albedo.

Globally, anthropogenic emissions of BC have increased more than fourfold since 1850, but emissions from North America, Europe and the former USSR have generally declined in recent decades (since the mid 20th century in America and Europe, and since 1990 in the former USSR (Ruppel, et al. 2014)). While the reduction in circum-Arctic emissions seems to have led to a return to near pre-industrial concentrations of BC in snow on Greenland, Ruppel, et al. (2014) show that ice cores from Svalbard have increasing concentrations of BC from 1970 to 2004, with concentrations in the most recent ice roughly four times higher than in pre-industrial ice.

A follow-up study (Ruppel, et al. 2017) suggests somewhat lower concentrations in firn deposited between 2006 and 2014, with significant interannual variability, but no clear negative trend. Ruppel, et al. (2017) also show that deposition is poorly modelled and not well correlated with atmospheric concentrations of BC. They suggest that deposition processes, which determine whether or not BC is moved from the air to the snow, play an important role and need further study. Ruppel, et al. (2014) suggest that increased flaring emissions from northern Russia may explain the increased BC concentrations in the latest decades captured in their core; it is possible that these emissions reach Svalbard but not Greenland. They also consider that wet scavenging efficiency may be higher due to the increased atmospheric temperatures observed over Svalbard.

4. Air temperature and precipitation

The recent increase in annual average temperatures over the Arctic is twice as large as the global average (AMAP 2012). There are large variations in the temperature development in the Arctic, and Svalbard is among the regions that have experienced the strongest warming in the last decades. It is

expected that the air temperature will continue to be affected by the anthropogenically caused increase in greenhouse gases, and that the temperature increase in Arctic areas will be twice the Northern Hemisphere average (AMAP 2017). There are larger uncertainties connected to the effect of global warming on precipitation development in the Arctic than for temperature. However, an increase in precipitation is expected over the Arctic as a consequence of the increased greenhouse effect (AMAP 2017). In addition, temperature and precipitation affect ecosystems and human activity and are therefore important climate indicators in the Arctic.

4.1 Air temperature

Air temperature measurements through 2016 from five Norwegian weather stations in the Arctic (Jan Mayen, Bjørnøya, Hopen, Svalbard Airport and Ny-Ålesund) are presented in Figure 7. The long-term temperature development at the five locations is quite similar. A temperature increase is seen at all stations in all seasons. There is large variability on both inter-annual and decadal scales. Colder periods are observed in the 1910s and 1960s and warmer periods in the 1930s and 1950s, in addition to the most recent warm period. The last decades are the warmest in the instrumental record. The five warmest years of the Svalbard Airport series all occur after 2005 (2006, 2007, 2012, 2014 and 2015). The warm years after year 2000 can also be observed in other Arctic regions (Overland, et al. 2015).

Linear trends are presented to quantify the temperature development. Positive trends are found for all stations and seasons, listed in Table 1a. The trend in the full-length annual time series of Svalbard Airport is significant on a 5% level (where a t-test is used as a significance test) and is 0.3 °C/decade, which gives a temperature increase of about 3 °C since 1900. This trend is about three times larger than the linear trend in the global annual mean temperature. This is consistent with IPCC which stated that the mean temperature increase will be larger in areas north of 65° N (Hartmann, et al. 2013). The seasonal trends from Svalbard Airport are all positive and significant at a 5% level. This is a change from the previous status report in MOSJ where the winter season did not have a statistically significant trend (Hansen 2010). The largest trends are found in winter and spring, both about 0.4 °C/decade.

The other temperature series give the same picture as Svalbard Airport. Because of the large inter-annual variability in the temperature series, the trends of each series depend on the start year. To enable comparison, linear trends for the last 40 years (1977−2016) are presented for all stations in Table 1b. The trends for this period are stronger than the trends for the full-length series, and also significant on a 5% level for all stations in all seasons. For the annual time series, linear trends up to 1.4 °C/decade are observed. In the seasonal series, the strongest warming is found in winter, with linear trends up to 2.5 °C/decade.

Table 1: Linear trends (°C/decade) for (a) full-length temperature series and (b) 1977–2016. Bold numbers indicate the trend is significant at the 5% level.

	a) Full-length						b) 1977–2016				
	Start year	Year	DJF	MAM	JJA	SON	Year	DJF	MAM	JJA	SON
Bjørnøya	1920	**0.16**	0.10	**0.32**	**0.10**	0.11	**0.91**	**1.57**	**0.81**	**0.44**	**0.78**
Hopen	1945	**0.45**	**0.66**	**0.54**	**0.26**	**0.35**	**1.39**	**2.47**	**1.31**	**0.49**	**1.14**
Svalbard Apt.	1898	**0.31**	**0.37**	**0.43**	**0.12**	**0.28**	**1.35**	**2.27**	**1.30**	**0.62**	**1.12**
Ny-Ålesund	1934	**0.22**	0.20	**0.37**	**0.13**	0.15	**1.01**	**1.88**	**0.92**	**0.38**	**0.76**
Jan Mayen	1921	**0.09**	0.04	**0.12**	**0.09**	0.09	**0.75**	**1.02**	**0.61**	**0.58**	**0.76**

Ny-Ålesund. Photo: M. König, Norwegian Polar Institute, 2018.

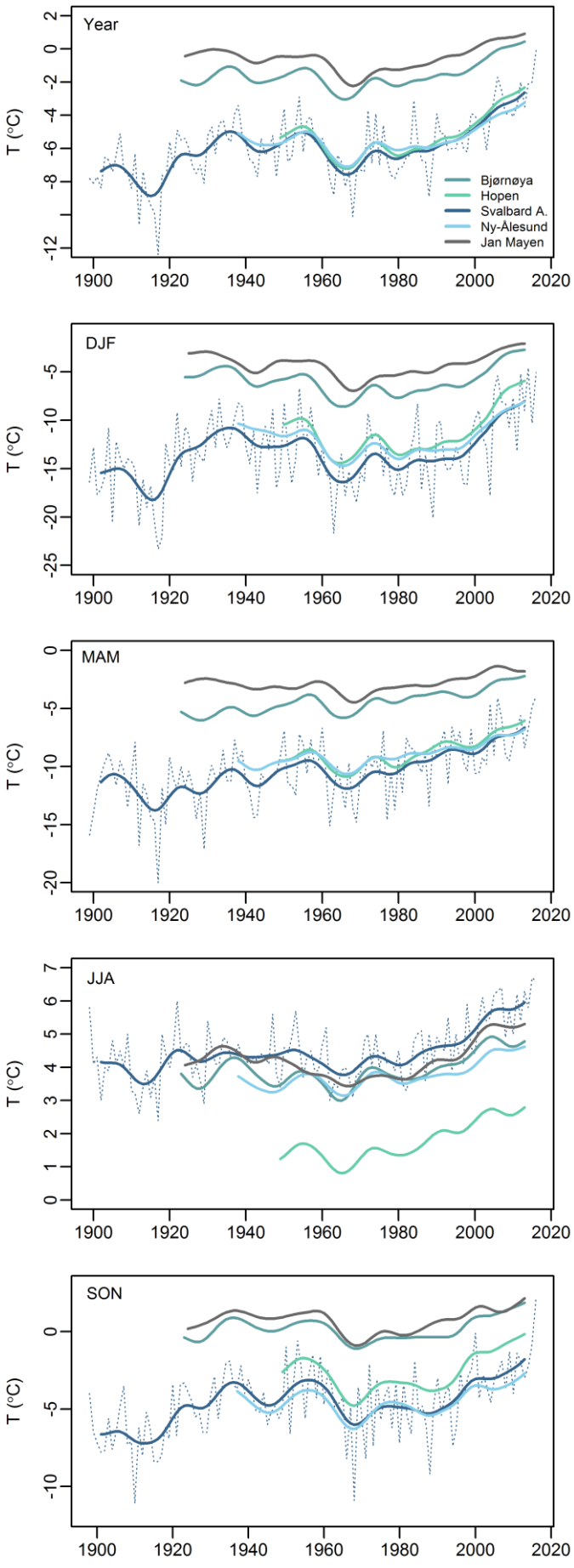

Figure 7: Long-term temperature development. Annual and seasonal homogenized temperature series from Bjørnøya, Hopen, Svalbard Airport, Ny-Ålesund and Jan Mayen. The series are smoothed with a Gaussian filter, highlighting longer-term variability. The three first and three last years of the filtered series have been excluded because the ends of such filtered curves have low certainty and changes when new values are added. The unfiltered series from Svalbard Airport (dotted line) is also included.

Threshold statistics show an increase in the number of warm days (daily mean temperature above 5 °C) per year and a decrease in the number of cold days (daily mean temperature below the 5th percentile) per year (Figure 8a, b). An absolute threshold could be used in summer because all stations have similar average summer temperatures; in winter, the stations have quite different average temperatures, so we used a percentile threshold. The decrease in cold days during the past 30 years is quite drastic. Bjørnøya, Hopen, Svalbard Airport and Ny-Ålesund observed no cold days in winter in 2012, 2014 and 2016. The observed change in cold days is larger than the observed change in warm days. This is connected to the larger wintertime warming. This difference is also observed in the extreme temperatures — the linear trend in minimum temperature over the past 30 years is about 0.3 °C per decade larger than the linear trend in maximum temperature. The larger warming in winter also leads to a decreasing intra-annual variability (Figure 8c), where most of the decrease is observed in winter and spring (Gjelten, et al. 2016).

There is a difference in warming between the stations. Svalbard Airport and Hopen show a stronger warming than the other stations (Table 1b). The temperature development at each station is closely linked to the development in local sea-ice cover (Isaksen, et al. 2016). The stations have seen a somewhat different development in the local sea-ice cover, and this is believed to be the main reason for the observed difference in warming between the stations in the past decades (Isaksen, et al. 2016).

The early 20th century warming in the Arctic is presumably caused by natural variability (Wood and Overland 2010). The temperature development in the period 1960–2000 may, to a large degree, be explained by changes in atmospheric circulation (Hanssen-Bauer and Førland 1998; Førland, et al. 2011). The most recent warming can be connected to changes in air mass characteristics and sea-ice extent, while changes in frequencies of atmospheric circulation types play only a minor role (Isaksen, et al. 2016).

Arctic air temperature is projected to increase throughout the 21st century. Benestad, et al. (2016) found that a 'typical warm winter' in 2099 over Fennoscandia and the high Arctic is estimated to be 7 °C warmer than a corresponding warm winter in 2010 (given the RCP4.5 emission scenario). Førland, et al. (2011) found that regional climate model simulations indicate a future rate in temperature increase in Svalbard three times stronger than in the observed series during 1912–2011. The strongest temperature increase is projected for the eastern and northeastern parts of the Svalbard region, where the sea-ice extent will be reduced (Figure 9a).

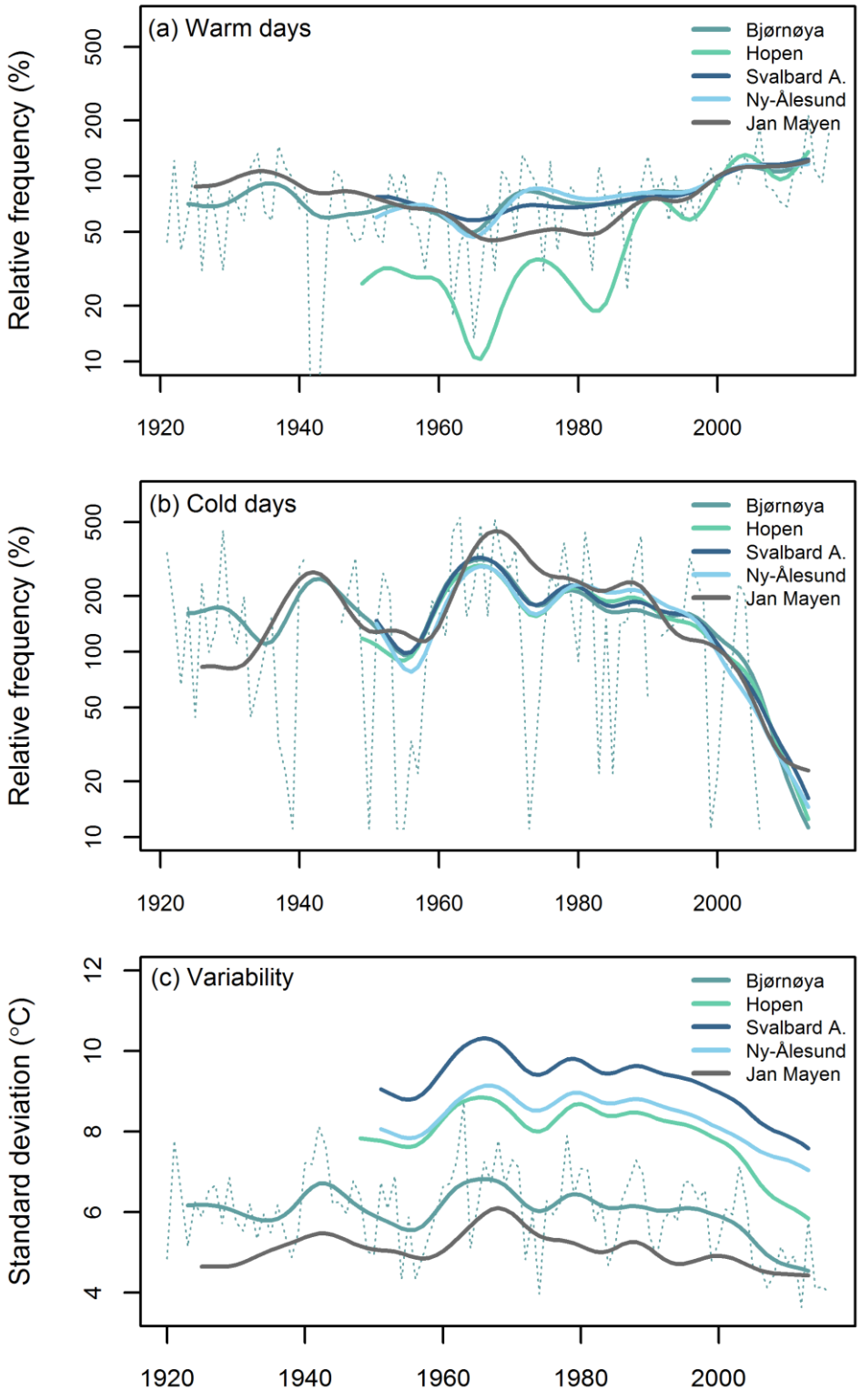

Figure 8: Development in number of cold and warm days per year and intra-annual variability. The series have been smoothed with a Gaussian filter, highlighting longer-term variability. The unfiltered series from Bjørnøya (dotted line) is also included. (a) Number of warm days (days with a daily mean temperature above 5 °C) per year for months MJJAS, relative to the 1987–2016 average. (b) Number of cold days (days with a daily mean temperature below the 5th percentile) per year for winter (NDJFM), relative to the 1987–2016 average. (c) Standard deviation (°C) of the daily mean temperature series each year.

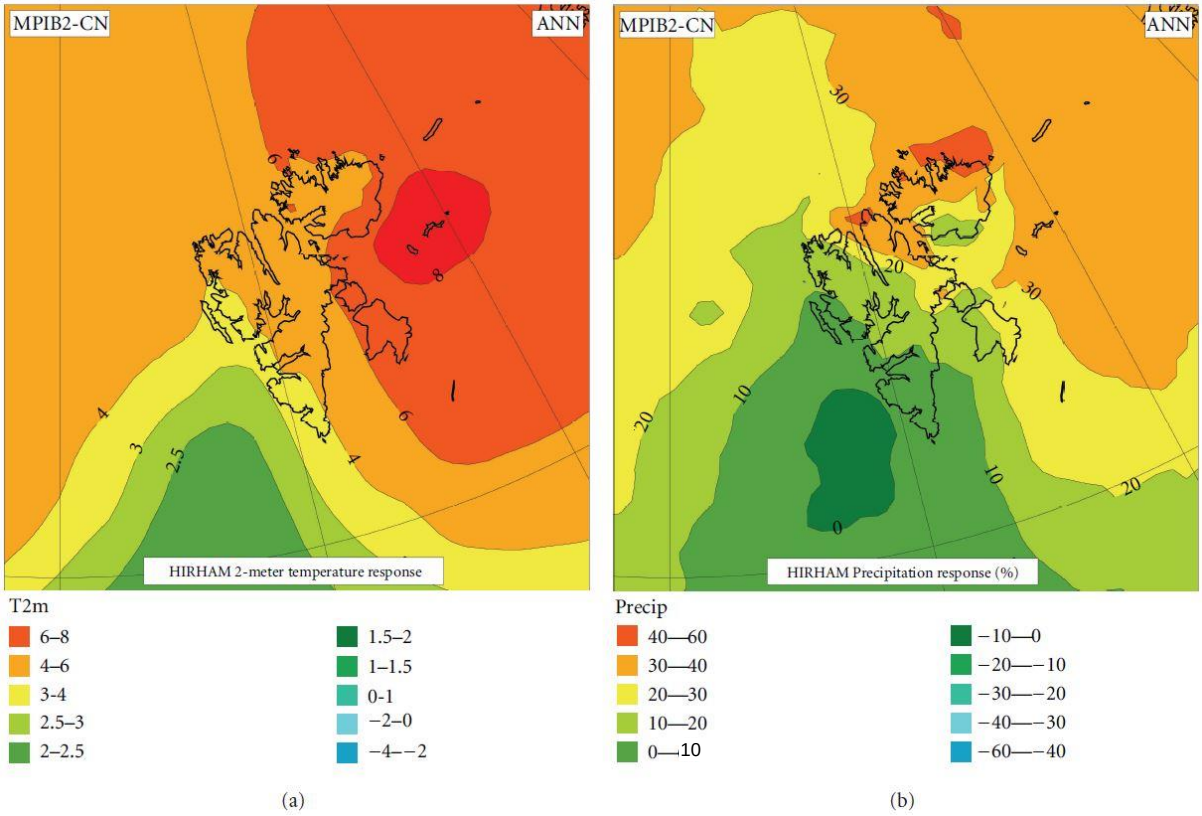

Figure 9: Projected changes from 1961–90 to 2071–2100 in (a) mean annual temperature (°C), and (b) mean annual precipitation (%). The figure is from Førland, et al. (2011).

4.2 Precipitation

The four stations examined here with long precipitation records show quite different development in annual precipitation sum on a decadal scale (Figure 10). However, all stations show a positive trend in the annual precipitation series even though the start years of the series are different (Table 2a). The trends for Bjørnøya, Svalbard Airport and Ny-Ålesund are statistically significant at a 5% level. Observations from Svalbard Airport show an increase in annual precipitation sum of about 6 mm per decade (3% per decade relative to the 1971–2000 average) since 1912. The trend for Jan Mayen is quite small (0.5%/decade) and not statistically significant.

The seasonal precipitation series show larger variation — there are positive and negative trends, and only a few of the trends are statistically significant. Jan Mayen shows negative trends in all seasons except autumn over the past 40 years (Table 2b). The Svalbard stations all show an increase in summer, autumn and winter over the past 40 years. The development in spring precipitation is very heterogeneous among the stations (Table 2b). It should be noted that Svalbard, and especially the Longyearbyen area, receives little precipitation compared to mainland Norway, so despite a large relative increase, the absolute increase in seasonal precipitation may just be a few mm.

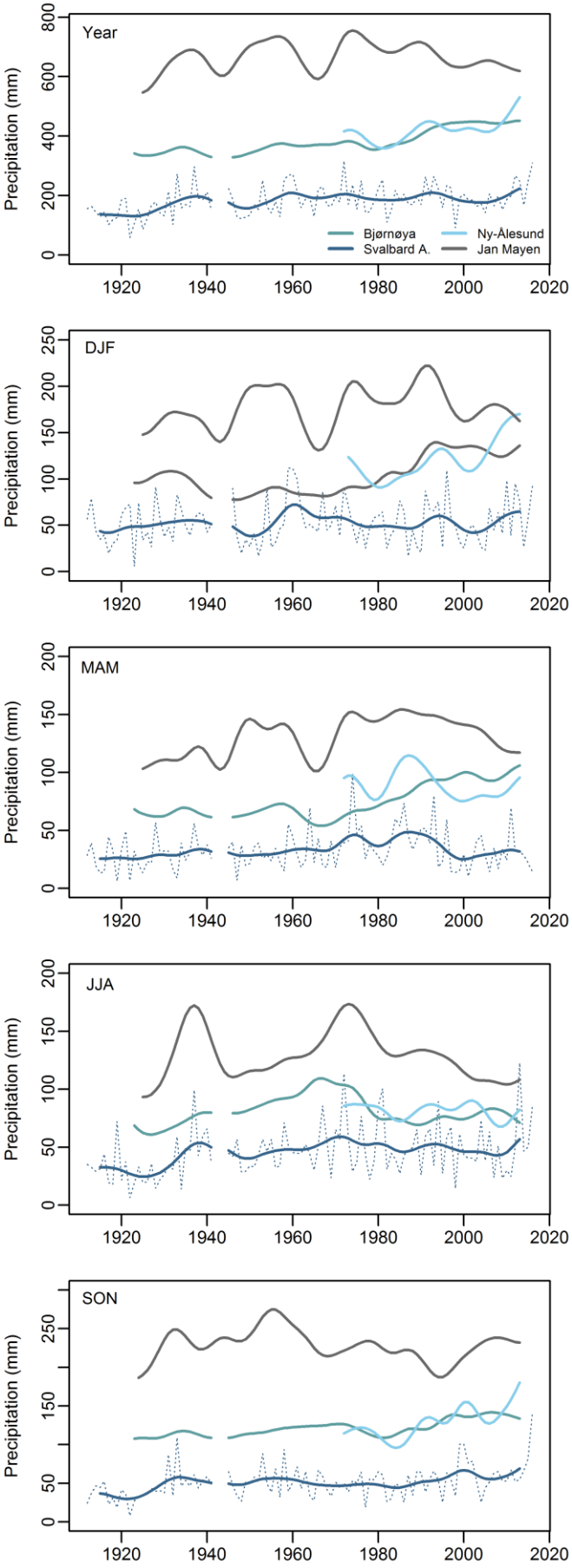

Figure 10: Annual and seasonal homogenized precipitation sums for Bjørnøya, Svalbard Airport, Ny-Ålesund and Jan Mayen. The data have been smoothed with a Gaussian filter, highlighting longer-term variability. The unfiltered series from Svalbard Airport (dotted line) is also included.

Occurrence of heavy precipitation events has increased over the past 60 years in Svalbard, but not on Jan Mayen (Figure 11a). For the period 1977–2016, Bjørnøya, Svalbard Airport and Ny-Ålesund show positive statistically significant trends between 10 and 17%/decade compared to the 1971–2000 mean, while Jan Mayen shows a negative trend of −5%/decade that is not significant.

Førland and Hanssen-Bauer (2003) attributed much of the observed long-term variations in precipitation in the 20th century to variations in atmospheric circulation, but uncertainties remain regarding attribution. Measuring precipitation in Arctic areas is challenging due to blowing and drifting snow and undercatch in the precipitation gauges. As the temperature has increased, the fraction of annual precipitation falling as snow has decreased. Because rain is easier to catch in the gauge than snow, part of the observed increase in precipitation is caused by a reduced undercatch in the precipitation gauges (Førland and Hanssen-Bauer 2000).

Table 2: Linear trends (%/decade, relative to the 1971–2000 mean) for a) full-length precipitation series, and b) 1977–2016.

	a) Full-length						b) 1977–2016				
	Start year	Year	DJF	MAM	JJA	SON	Year	DJF	MAM	JJA	SON
Bjørnøya	1920	**3.1**	**4.4**	**5.2**	0.1	**2.5**	**8.0**	**11.2**	**12.7**	1.2	6.7
Svalbard Apt.	1912	**3.1**	1.4	2.0	**4.2**	**4.7**	5.1	7.8	-9.1	2.9	**16.4**
Ny-Ålesund	1969	**7.5**	11.5	-0.2	-0.9	**14.7**	**12.1**	**19.7**	0.7	1.8	**20.2**
Jan Mayen	1921	0.5	1.1	2.0	-0.4	-0.1	**-3.3**	-3.8	-6.0	**-7.1**	1.7

Arctic precipitation is projected to increase through the 21st century. There are large uncertainties connected to the size of the projected increase, but perhaps up to 50%. The changes are connected to larger atmospheric moisture content because of warmer air and evaporation from larger areas as sea-ice retreats. The temperature increase of the air masses also affects the precipitation amount (Benestad, et al. 2016; Bintanja and Selten 2014; Førland, et al. 2011; Koenigk, et al. 2015). Førland, et al. (2011) showed that regional climate model simulations project an increase in precipitation and heavy precipitation events in Svalbard up to year 2100. The projected increase in mean annual precipitation ranges from a few percent southwest of Spitsbergen to more than 40% in north-eastern parts of the archipelago (Figure 9b). This spatial pattern is similar to the temperature pattern, reflecting that temperature increases lead to precipitable water increases, which in turn allow for more precipitation.

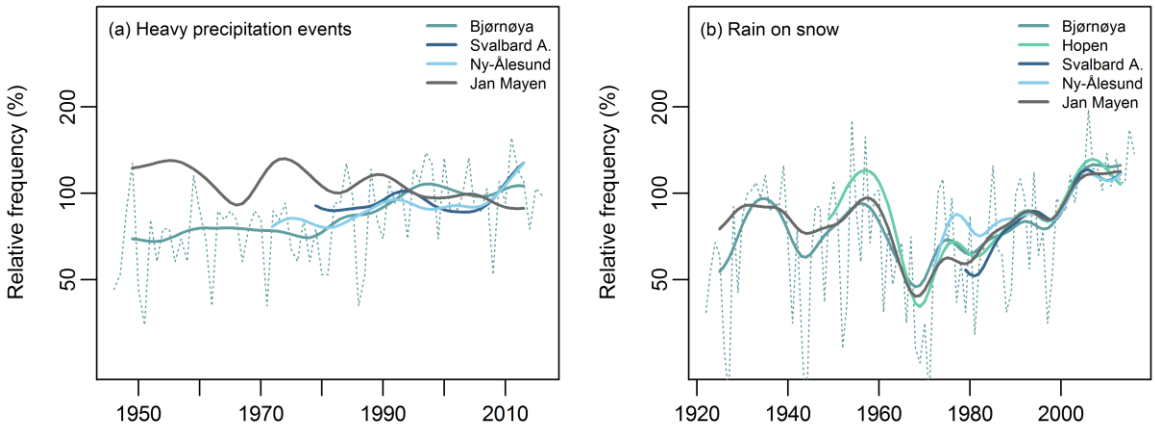

Figure 11: Number of days per year, relative to the 1987–2016 mean, with (a) a precipitation sum above the 95th percentile, and (b) observed precipitation and a daily mean temperature above 0 °C during the winter season (NDJFMA). The series have been filtered with a Gaussian, filter revealing the decadal variation. The unfiltered series from Bjørnøya (dotted line) is also included.

Note: Only the monthly precipitation series are homogenized. Daily precipitation data from Bjørnøya and Jan Mayen before 1947 is excluded because of homogeneity breaks. The precipitation series from Hopen is not presented at all because of large inhomogeneities in the series.

4.3 Winter warming events

There have been reports of extreme winter warming events in the Arctic in the recent years (Graham, et al. 2017a). These events are characterized by extraordinarily warm weather episodes, occasionally combined with intense rainfall (Hansen, et al. 2014; Vikhamar-Schuler, et al. 2016). Rain-on-snow (ROS) events in winter have increased in the last 50 years (Figure 11b). The development follows the general long-term temperature development (Figure 7) with increased frequency of ROS events during warmer periods in the 1930s and 1950s and a general increase in frequency over the past 50 years.

Vikhamar-Schuler, et al. (2016) show that extreme winter warming events are expected to increase throughout the 21st century up to two or three times larger than the current level. The enhanced warming in the Arctic is of great concern as more winter warming events and, in particular, more frequent and intensified ROS events can have major impact on, for example, wildlife, transportation and infrastructure in Arctic areas.

5. Snow cover

Arctic snow cover is responding to multiple environmental drivers and feedbacks, such as warming, increased moisture availability, changing atmospheric circulation, changing vegetation, increased frequency of winter thaws and rain-on-snow events (Brown, et al. 2017). Recent studies suggest widely varying snowfall trends across the Arctic, depending on climate regime (Vihma, et al. 2016). Negative trends in snowfall are observed in regions with warmer winter climates such as Scandinavia (Rasmus, et al. 2015; Irannezhad, et al. 2016) while increasing snowfall is documented in cold

regions such as northern Canada and Siberia (Kononova 2012; Vincent, et al. 2015). According to Brown, et al. (2017), there is widespread multi-dataset evidence of reductions in annual snow cover duration over Arctic regions at rates ranging from −2 to −4 days/decade over the past 30−40 years, with the largest decreases observed in the warmer sectors of the Arctic. The European sector of the Arctic shows consistent negative trends in annual maximum snow accumulation across all data sources (Brown, et al. 2017).

In Svalbard and on Jan Mayen several long-term time series of precipitation exist (see chapter on air temperature and precipitation). Solid precipitation is the principal input to a snow cover. However, solid precipitation and snow measurements in Svalbard and Jan Mayen are strongly influenced by wind-induced bias, which may cause fictitious trends (Førland and Hanssen-Bauer 2000). At the Norwegian Arctic stations, drifting or blowing snow occasionally cause substantial problems. For instance there is often a combination of precipitation and blowing snow. In such cases it is difficult to distinguish the proportions of real precipitation and blowing snow (Førland and Hanssen-Bauer 2000). In addition, in situ observations are subject to many other site and gauge issues (e.g. reporting of trace precipitation, station shifts, changes in measurement protocols, automation). Thus, obtaining reliable estimates of solid precipitation trends is a challenge (Brown, et al. 2017).

An interesting measure of long-term precipitation trends related to snow cover is the annual fraction of solid precipitation (Førland and Hanssen-Bauer 2000). The long-term manned series from Jan Mayen, Bjørnøya and Spitsbergen exhibit large year-to-year variations in solid precipitation fraction, as shown in Figure 12; e.g., during 1975–2016 the fraction falling as solid precipitation at Ny-Ålesund varied between 19% (2016) and 69% (1998). A significant negative trend for the annual fraction of precipitation falling as snow was found at all four stations, with −11% per decade at Jan Mayen, −5% per decade at Bjørnøya, −11% per decade at Svalbard Airport and –8% per decade at Ny-Ålesund. The conversion from snow to mixed precipitation and rain is mainly a consequence of the increase in air temperature during the last decades.

*Ice-covered vegetation and a Svalbard rock ptarmigan (*Lagopus muta hyperborea*) in Svalbard.*
Photo: E. Fuglei, Norwegian Polar Institute, 2015.

The annual snow-cover duration (number of days with measurable snow cover at the station's snow-depth observation location) has varied widely among the stations on Jan Mayen and in Svalbard during the last couple of years (Figure 13). In general, the stations have 191 to 273 days throughout the year where the ground is covered with snow. The year 2016 was a particularly mild year, and Ny-Ålesund and Jan Mayen had the shortest duration in the series, while Svalbard Airport had the third shortest (2007 and 2011 were lower). Due to several gaps in the data series (Figure 13), it is challenging to compare the development of snow-cover duration between the Norwegian Arctic stations and it has not been possible to perform robust testing of statistical significance of trends. In general, datasets show that there is large inter-annual variability. Jan Mayen has a large gap in the series which, along with the large natural inter-annual variability, makes it hard to see any clear trend. Svalbard airport has the largest data coverage and shows a clear tendency for fewer days of snow cover since 2006 compared with the 1970s and 1980s. In the end of the 1970s, the number of days of snow cover per year was approximately 255, while the last five years are ~225 days (Figure 13).

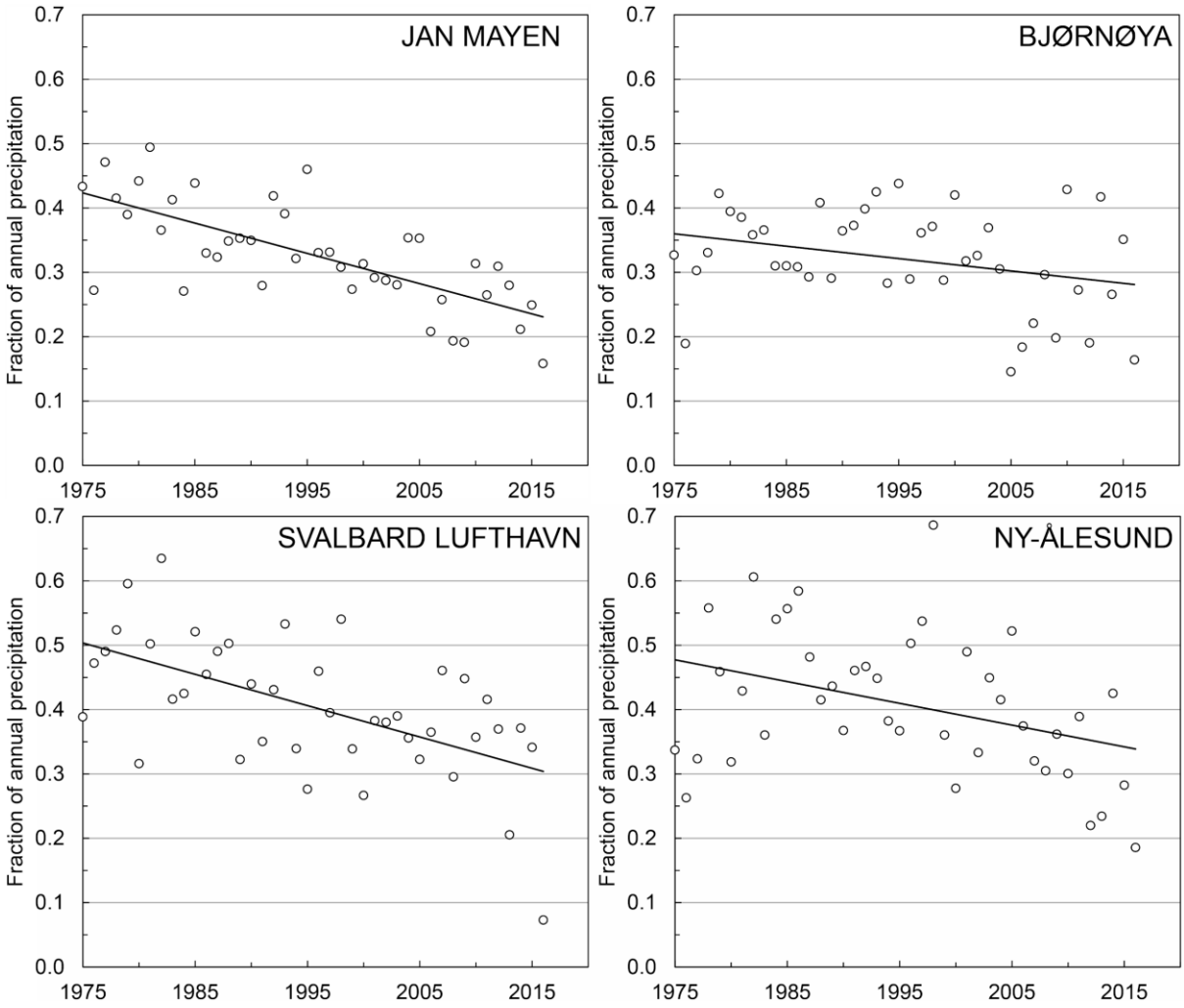

Figure 12: Annual fractions of solid precipitation measured at Jan Mayen, Bjørnøya, Svalbard Airport and Ny-Ålesund 1975–2016. The solid lines indicate linear trends. Modified and updated after Førland and Hanssen-Bauer (2000).

Van Pelt, et al. (2016) analysed trends and spatial variability of snow-related parameters over Svalbard for the period 1961–2012, based on a High Resolution Limited Area Model (HIRLAM), downscaled onto a 1-km Snow-Model grid and validated against snow depth data on 13 glaciers around Svalbard. In response to autumn warming, van Pelt, et al. (2016) found that the date of snow onset increased (two days per decade), whereas in spring/summer opposing effects of earlier melt onset and higher winter accumulation caused a nonsignificant trend in the date of snow disappearance. Maximum snow water equivalent (SWE) in winter/spring shows a modest increase (+0.01 m water equivalent per decade), while the end-of-summer minimum snow-area fraction declined from 48% to 36%. The perennial snow fraction is governed by both winter accumulation and summer melt and showed a significant negative trend of −0.02 per decade (van Pelt, et al. 2016).

Analyses from a regional climate model for the high greenhouse gas emissions scenario RCP8.5 over Svalbard show that, by the end of the century, during winter nearly all precipitation on average will still fall as snow inland and at higher elevations, but closer to the west coast, an increasing proportion of precipitation will fall as rain (Isaksen, et al. 2017). The increase in snowfall may increase the maximum snow depth in the inner parts of Svalbard, where the average temperature is still well below freezing in winter. The average snow depth will generally decrease, but the results also show a certain increase inland in winter.

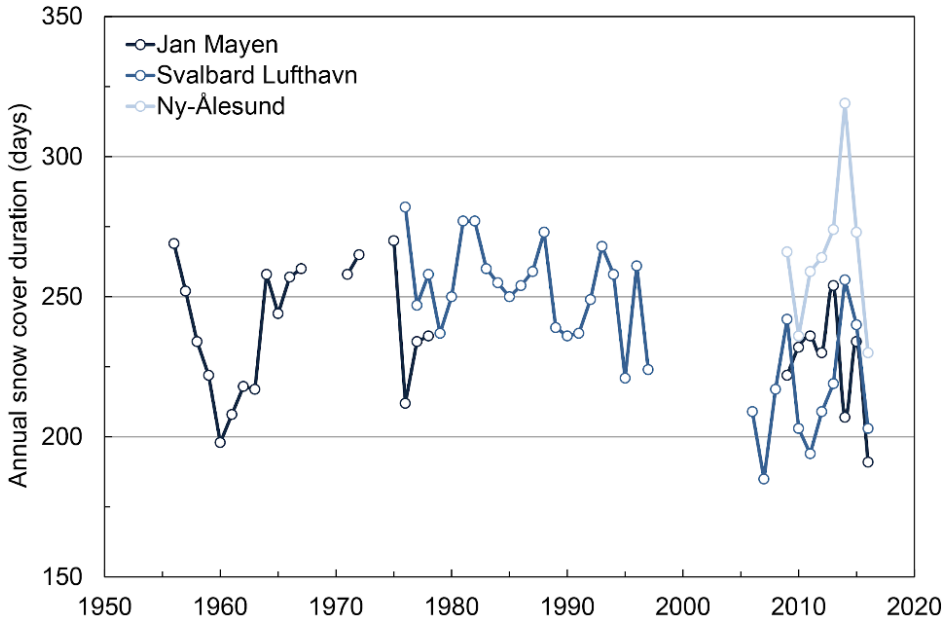

Figure 13: The annual snow cover duration observed at the manned weather stations Jan Mayen, Svalbard Airport and Ny-Ålesund.

6. Permafrost

Permafrost, or permanently frozen ground, consists of soil or rock and included ice and organic material that remains at or below 0 °C for at least two consecutive years. About a quarter of the exposed land surface of the Northern Hemisphere is underlain by permafrost (Zhang, et al. 2003). The most direct indicators of changes in the thermal state of permafrost are permafrost temperature and active-layer thickness. Permafrost temperature measured at a depth where there is practically no annual fluctuation in ground temperature is the best indicator of long-term change. This depth varies from a few metres in warm, ice-rich permafrost to 20 m or more in cold permafrost and in bedrock (Romanovsky, et al. 2010; Smith, et al. 2010).

In recent years, new record high mean annual ground temperatures have been observed at many permafrost observatories across the Arctic (Romanovsky, et al. 2017). The greatest temperature increase occurred in the colder permafrost of the Arctic and High Arctic. In warmer permafrost, the temperature increase has been much less or not detectable (Romanovsky, et al. 2017). Most of the regions where long-term observations of active-layer thickness (the top layer of soil that thaws during summer and refreezes in winter) are available show an increase in active-layer depth over the past five years. During the past 30 years, the average date of freeze-up of the active layer in northern Alaska has become almost two months later. At some locations (such as in northern European Russia) permafrost degradation (reduction in thickness and/or lateral extent) has been observed (Romanovsky, et al. 2017).

One of the most dramatic results of thawing permafrost is the potential mobilization of the organic material currently sequestered in perennially frozen deposits (Schuur, et al. 2008; 2015). The potential release of carbon dioxide (CO_2) and methane (CH_4) from thawing permafrost may have not only regional but also global impacts on climate (Koven, et al. 2015) by enhancing the increasing concentration of these gases, shown in the section above on greenhouse gases.

Ground temperature records in Svalbard from monitoring at Kapp Linné (on the western coast of Spitsbergen) and Janssonhaugen (in the central part of the valley Adventdalen in Spitsbergen) show that ground temperatures at 20 m depth are increasing by about 0.7 °C per decade (Figure 14). Strand (2016) found that between 2010 and 2015 ground temperature at 10 m depth at three other monitoring sites nearby Longyearbyen (the Old Auroral Station in Adventdalen, in Endalen and at Breinosa) has increased between 0.3 °C and 0.9 °C, over the six year period. Over the same period the ground temperature at 10m depth on Janssonhaugen increased by approximately 0.4 °C.

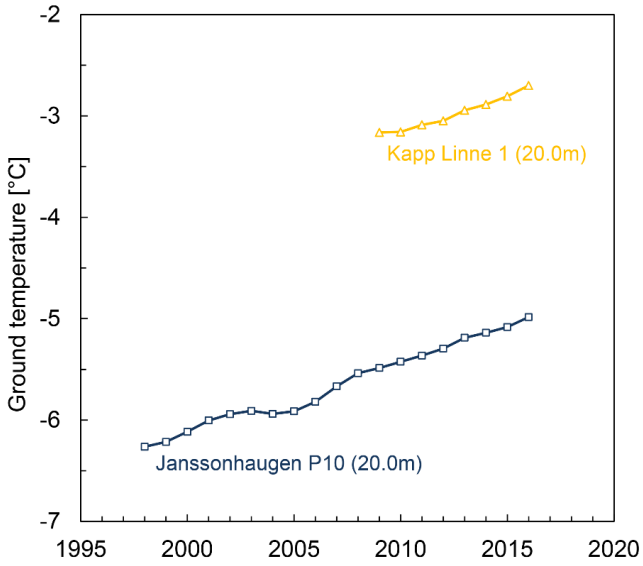

Figure 14: Time series of mean annual ground temperature at 20 m depth below the surface at Kapp Linné on the western coast of Spitsbergen and Janssonhaugen, in the central part of the valley Adventdalen on Spitsbergen. Data series are updated from Isaksen, et al. (2007) and Christiansen, et al. (2010).

On Janssonhaugen, a significant temperature increase is measureable down to at least 80 m depth (Figure 15) reflecting a multi-decadal warming of the permafrost surface, with 2016 clearly as the most extreme year in the observational record.

Active-layer-thickness (ALT) records from Janssonhaugen indicate a general increase of about 0.3 m in ALT since 1999. ALT in 2016 on Janssonhaugen was about 2 m, 15% thicker than the 2000–2015 mean and was the highest in the entire 1998–2016 observational record (Figure 16).

To study expected changes by the end of the century, Etzelmuller, et al. (2011) used results from a multi-model GCM ensemble to derive ground surface temperature series for driving a ground heat conduction model for individual borehole locations on Spitsbergen. The models were forced with the so-called SRES A1b emissions scenario (in which atmospheric CO_2 reaches 720 ppm by 2100). The ground temperature calculations for the borehole sites at Kapp Linné, Janssonhaugen, Endalen and Gruvefjellet revealed the following major effects on the permafrost thermal state by the end of the century (Etzelmüller, et al. 2011):

1. A significant warming (ca. +4 °C) in the near-surface layers (<10 m depth) is calculated.
2. The temperature increase varies depending on ice/water content and thermal state today.
3. Warming rates are efficiently reduced where the temperature is close to 0 °C and ice is present, due to the consumption of latent heat for melting.
4. The median ground temperature at the depth of zero annual amplitude is expected to increase by 2–4 °C, over the period 2000–2100.
5. Over the same period, ALT increases at all sites; the magnitudes of the modelled increase depend on ground surface temperature and ground characteristics. Model results show degradation of permafrost in bedrock sites at low elevations; however, in sedimentary landforms with a relatively high water/ice content, permafrost conditions continue to exist until 2100.

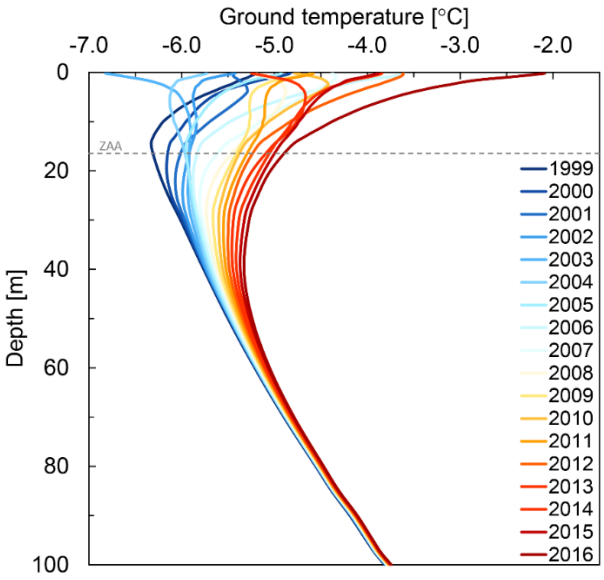

Figure 15: Mean annual ground temperature profiles on permafrost monitoring site Janssonhaugen, Svalbard from 1999 to 2016. The depth of zero annual amplitude is marked by a grey dotted line.

Recent ground thermal calculations made by Instanes and Rongved (2017), based on regional climate model runs using the RCP4.5 emissions scenario, suggest an ALT increase in Longyearbyen from about 1.5 m today to about 2.5 m by the end of the century. Due to high ice content, warming rates are efficiently reduced. By 2100, the calculations suggest that the temperature at 20 m will still be −2 to −3 ° C. Although the calculations show that there will still be permafrost in Longyearbyen until after 2100 under the RCP4.5 scenario, the increased ground temperatures will cause poorer bearing capacity of foundations. This must be taken into account in future planning and engineering of new buildings and installations in Svalbard (Instanes and Rongved 2017).

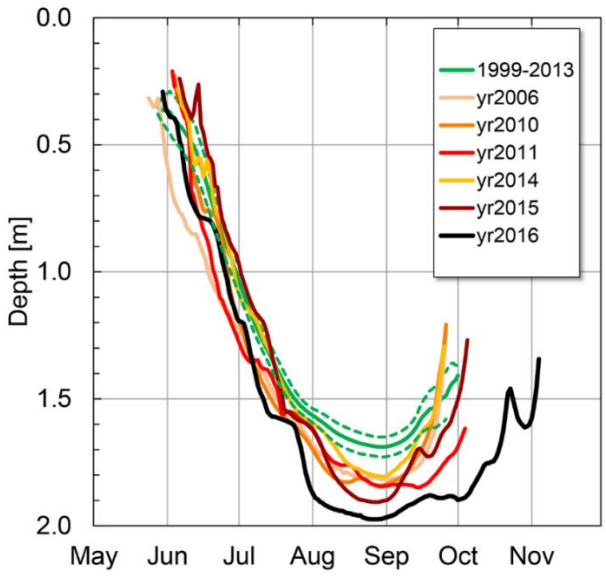

Figure 16: Daily calculated depth of 0 °C isotherm, reflecting the active layer thickness for selected years on Janssonhaugen. The 1999 to 2013 average is in green. The dotted line around the average line shows the one standard deviation range of the data.

7. Glaciers

Mass loss from the world's "small" glaciers, that is, all ice bodies apart from the Greenland and Antarctica ice sheets, is one of the main contributors to current sea-level rise (Gardner, et al. 2013). Furthermore, fresh water from glacier melt is an important component in the hydrological cycle, affecting ecosystems and ocean flow. Accordingly, glaciologists seek to estimate the mass balance in all glaciated regions of the world.

Glacier mass balance is the amount of snow and ice lost or gained on a glacier over a certain period. It is usually reported as a single number which reflects the average loss or gain for the glacier as a whole. It represents a lumped climate signal that is influenced primarily by winter precipitation and summer temperature.

Svalbard is ~60% glacier-covered (König, et al. 2014), and comprises ~10% of the total Arctic glacier area. Svalbard glaciers as a whole are retreating, based on long-term records of front positions (Nuth, et al. 2013; König, et al. 2014). The short-term exception to this general pattern of retreat is seen for Svalbard's many surge-type glaciers, which alternate long periods of relative dynamic quiescence with short duration advances that last 1–3 years, in which the glacier speeds increase dramatically and the glacier front advances, sometimes by kilometres or more. However, once the surge is over, retreat continues. Furthermore, during the surge, there is no gain of mass; ice is simply shifted downglacier, to lower elevations, where melting is greater. While front position data are, therefore, not the ideal metric for deducing change, there is abundant evidence from field measurements, modelling, and remote sensing data, described in more detail below, that Svalbard glaciers are losing mass, as one would suspect from the marked frontal retreats.

Summer temperature has the strongest influence on Svalbard glacier mass loss (van Pelt, et al. 2012), and decadal-scale Arctic summer warming has led to increasing rates of mass loss (Kohler, et al. 2007). With further Arctic warming (Collins, et al. 2013; Førland, et al. 2011), Svalbard glaciers can be expected to continue to lose mass (Lang, et al. 2015).

7.1 Glaciological mass balance

The glaciological mass balance is obtained from regular field visits to a few selected glaciers. Field data collected in spring and autumn are used to derive winter and summer balances (B_w and B_s), which when summed yield the annual mass balance B_n.

An additional mass balance component is the dynamic loss at the front of tidewater glaciers, that is, glaciers that terminate in seawater and lose ice by calving. About 60% of Svalbard's total glacier area drains through tidewater fronts (Błaszczyk, et al. 2009), such that a significant part of the total ice mass loss occurs via calving. Warmer ocean water around Svalbard, in combination with the overall atmospheric warming, contributes strongly to the retreat of Svalbard's tidewater glaciers (Luckman, et al. 2015). Svalbard-wide calving has been estimated to be 0.13 metres water equivalent per year (w.eq./yr), averaged across Svalbard's ~34,000 km^2 of glaciers (Błaszczyk, et al. 2009).

There are a number of field monitoring programmes of mass balance around Svalbard, most of which are in the Kongsfjorden area (Figure 17, Table 3). Here we only consider time-series with continuous records five years or longer. The longest-term field measurements of mass balance in Svalbard are on the two small glaciers Austre Brøggerbreen and Midtre Lovénbreen (Table 3). Data show that both glaciers had consistently negative mass balances since the beginning of their records (Figure 18). Midtre Lovénbreen has a slightly less negative net balance than the neighboring Austre Brøggerbreen, due in part to topography; the slightly higher elevation of the former glacier and its steeper valley sides both contribute to more accumulation in its upper part. Similarly, larger glaciers, such as Kongsvegen (Figure 17), have a more positive mass balance than small ones (Figure 18), since larger glaciers usually extend to higher elevations, and therefore have significantly larger accumulation areas.

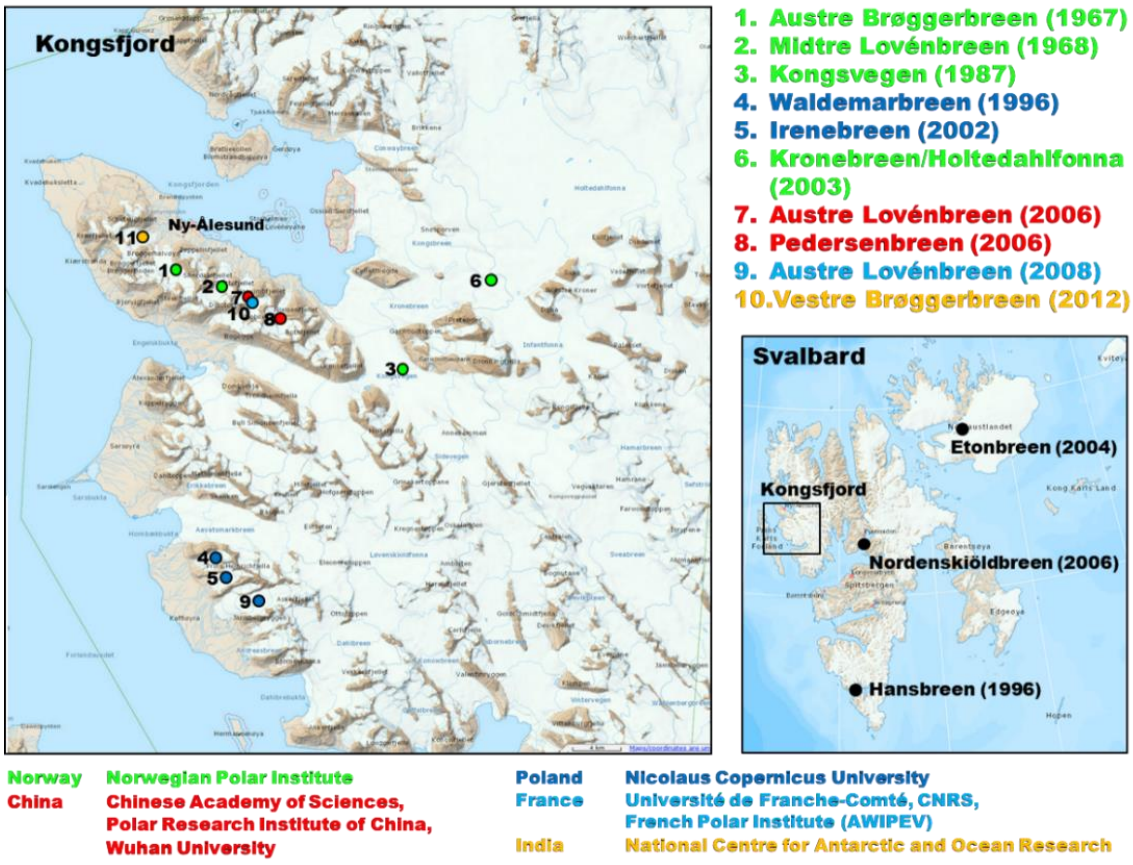

Figure 17: Location of mass balance studies in the Ny-Ålesund area.

Winter accumulation is less variable than summer ablation, with the latter contributing more variability to the net balance (Figure 18). While trends for both winter and summer balances are not statistically significant, there is an overall tendency over the measurement periods for decreased winter accumulation and increased summer melting. The long-term cumulatively summed net mass balance, which is roughly equivalent to the volume change, shows that over the long term, these glaciers are losing mass (Figure 18).

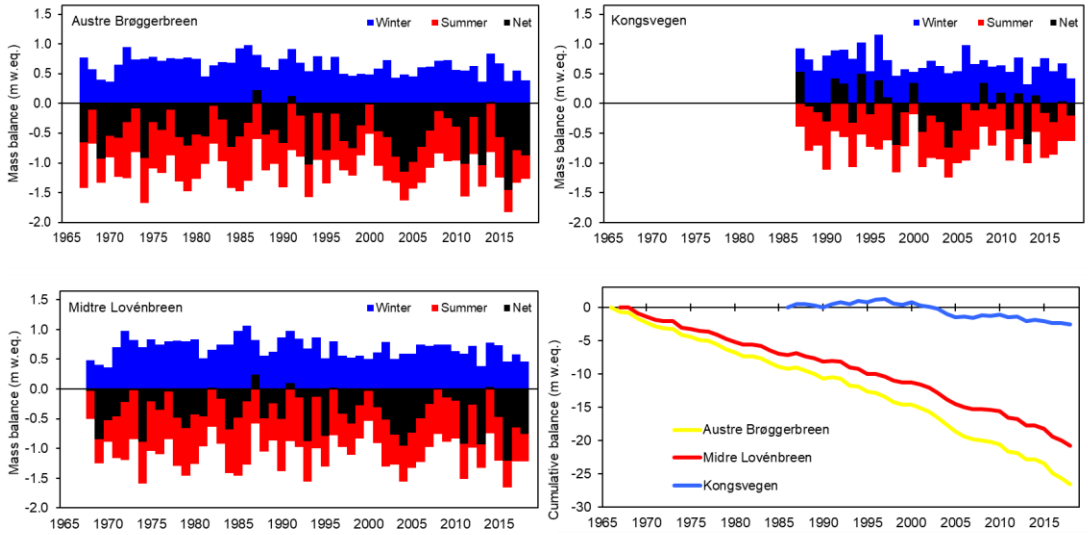

Figure 18: Winter, summer and net balance record from Brøggerbreen, Midtre Lovénbreen and Kongsvegen. The blue bars show the total accumulation on the glacier during the accumulation season, converted to an area average thickness of water (metres of water equivalent, m w.eq.); red bars similarly show the net melt over the melt season, while black bars are the sum of the two, or the total gained or lost to surface processes over the year. The effect of calving on total mass balance is included by adding the transparent grey bars to the black bars.

Table 3: Long-term continuing glacier mass balance measurements around Svalbard. NPI: Norwegian Polar Institute; PAS: Polish Academy of Science; UNC: University of Nicolaus Copernicus, Poland; UiO: University of Oslo; UUS: Uppsala University, Sweden; UUN; Utrecht University, Netherlands; PRIC: Polar Research Institute of China; CAS: Chinese Academy of Science; CNRS: French National Centre for Scientific Research; NCAOR: National Centre for Antarctic and Oceanographic Research, India. Areas and elevation ranges are taken from most recent version of the Svalbard Glacier Database, covering the 2000s (Nuth, et al. 2013).

Glacier	Agency	Region	Area (km^2)	Elevation range (masl)	Years
Austre Brøggerbreen	NPI	Kongsfjorden	5.8	80–680	1967–present
Midtre Lovénbreen	NPI	Kongsfjorden	5.1	50–690	1968–present
Kongsvegen	NPI	Kongsfjorden	106.9	0–1000	1987–present
Hansbreen	PAS	Hornsund	63.4	0–695	1989–present
Waldemarbreen	UNC	Kaffiøyra	2.7	140–590	1996–present
Irenebreen	UNC	Kaffiøyra	3.4	110–780	2002–present
Kronebreen-Holtedahlfonna	NPI	Kongsfjorden	380.0	0–1400	2003–present
Etonbreen	NPI/UiO	Nordaustland	633.0	0–800	2004–present
Nordenskiöldbreen	UU/UU	Billefjorden	141.2	0–1230	2006–present
Austre Lovénbreen	PRIC/CAS	Kongsfjorden	5.0	95–650	2006–present
Pedersenbreen	PRIC/CAS	Kongsfjorden	6.1	50–790	2006–present
Austre Lovénbreen	CNRS	Kongsfjorden	5.0	95–650	2008–present
Vestre Brøggerbreen	NCAOR	Kongsfjorden	4.6	50–580	2012–present

7.2 Geodetic mass balance

The geodetic mass balance is computed by differencing glacier-wide elevation data from two or more different times. Elevation data can be from a variety of sources: surface surveys; contours from older maps; digital elevation models made photogrammetrically from aerial photographs or satellite imagery; or satellite altimeters.

While the glaciological mass balance is accurate in describing short-term glacier changes on individual glaciers, it becomes less accurate when summed over time. In contrast, the geodetic mass balance is more accurate over longer periods and the necessary data can be acquired over larger areas. However, only recently has it been possible to collect Svalbard-wide elevation data within a single year, mostly due to advances made in satellite remote sensing.

Nuth, et al. (2010) compared satellite altimetry data from the Ice, Cloud, and Land Elevation Satellite (ICESat) mission for the period 2003–2007 to older topographic maps and digital elevation models for different epochs (1965–1990). Because the ICESat tracks are relatively sparsely distributed, they extrapolate along-track changes to the larger regions using the glacier hypsometry. Nuth, et al. (2010) find significant thinning at the lower elevations of most glaciers, and either slight thinning or thickening in the accumulation areas, except for glaciers that surged during the observation period; these glaciers show thickening in the ablation area and thinning in the accumulation areas. However, the overall balance is very negative at −0.36 m w.eq./yr, corresponding to −9.7 Gt/yr. This estimate excludes Austfonna and Kvitøya, and is averaged over different periods for different geographic regions. The most negative geodetic balances are found in the south and the least negative balances in the northeast.

Moholdt, et al. (2010) determined elevation changes along the ICESat tracks for the period 2003–2008, extrapolating these changes to the remaining glacier area using the same hypsometric approach as Nuth, et al. (2010) to yield a Svalbard-wide estimate of −0.12 m w.eq./yr, or −4.3 Gt/yr. Similarly to Nuth et al, they find that most regions experienced low-elevation thinning and high-elevation balance or thickening, and that the largest ice losses occurred in the west and south, while northeastern Spitsbergen and the Austfonna ice cap gained mass.

Analysis of older maps and modern DEMs (Kohler, et al. 2007) of a few selected glaciers in western Svalbard shows that the rate at which these glaciers lost mass appears to have accelerated over time. For example, the average thinning rate for Midtre Lovénbreen, the glacier with the best cartographic data, increased steadily since 1936. Thinning rates for 2003−2005, the most recent period analysed (Kohler, et al. 2007), were more than four times the average for the first measurement period 1936−1962. On Slakbreen, south of Longyearbyen, thinning rates for the period 1990−2003 were more than four times that of the period 1961−1977 (Kohler, et al. 2007). James, et al. (2012) found a similar increase in thinning rates for other glaciers around Svalbard. A trend of increasingly negative mass balance is consistent with both worldwide glacier trends, as well as developments in the Arctic climate (Kaser, et al. 2006).

Table 4: Svalbard-wide long-term net glacier mass balance using different methods.

Reference	Period	Specific B_n (m w.eq./yr)	B_n (Gt/yr)	Method
(Nuth, et al. 2010)	(1965−1990) to (2003 −2007) (period varies geographically, and excludes Austfonna, Kvitøya)	−0.36 ± 0.02	−9.7 ± 0.55	Geodetic
(Moholdt, et al. 2010)	2003−2008	−0.12 ± 0.04	−4.3 ± 1.4	Geodetic
Aas, et al., 2016	2003−2013	−0.26 −0.39	−8.7 −13.3	Model Model + calving
Østby et al., 2017	2004−2013	−0.20 −0.33	−6.8 −11.2	Model Model + calving
Wouters et al., 2008	2003−2008	−0.26 ± 0.09	−8.8 ± 3	GRACE
Jacob et al., 2012	2003−2010	−0.09 ± 0.06	−3 ± 2	GRACE
Mémin et al. 2011	2003−2009 2003−2009	−0.27 ± 0.03 −0.46 ± 0.07	−9.1 ± 1.1 −15.5 ± 2.4	GRACE method 1 GRACE method 2
Matsuo and Heki, 2013	2004–2012 2004−2008	−0.11 ± 0.09 −0.20 ± 0.11	−3.6 ± 2.9 −6.9 ± 3.6	GRACE
(Gardner, et al. 2013)	2003−2009 2003−2009	−0.20 ± 0.06 −0.13 ± 0.12	−7 ± 2 −5 ± 4	GRACE Method A GRACE Method B

7.3 Mass balance modelling

Measuring mass balance in the field is expensive, and therefore limited to only a few locations. Data from these few glaciers can be extrapolated to larger areas or regions (Hagen, et al. 2003), but field measurements of mass balance are more advantageously used together with mass balance models. Climatic mass balance models, forced either by meteorological observations or output from regional climate models, evaluate the surface energy balance to determine surface temperature and melt production. The most physically complete models couple the surface module to subsurface layer-tracking routines to account for the impact of water storage and refreezing on the mass and energy budgets. Field data are used to calibrate model parameters and to validate model output.

There are at present only a few studies modelling historical Svalbard-wide mass balance using fully physical models, as opposed to statistical (Day, et al. 2012) or temperature-index (Möller, et al. 2016) approaches. Aas, et al. (2016) perform a mass balance simulation for all of Svalbard over the period 2003–2013, using field data for model calibration. They find a strongly negative average mass balance of −0.26 m w.eq./yr, or −8.7 Gt/yr. Using a different model and climatic forcing, Østby, et al. (2017) simulate mass balance over the longer period 1957−2014. They find that Svalbard cumulative net balance was slightly positive for the whole period, but that the trend was significantly negative, with a shift from positive balance to negative occurring around 1980. The average for the most recent model period 2004–2013 is strongly negative at −0.20 m w.eq./yr, or 6.8 Gt/yr. Both models are for the climatic mass balance only; when the estimated Svalbard-wide calving amount of −0.13 m w.eq./yr (Błaszczyk, et al. 2009) is included, the overall Svalbard mass balance estimated is even more negative (Table 4).

7.4 Gravity

The GRACE (Gravity Recovery and Climate Experiment) satellite mapped the time-varying gravity field of the Earth over the period 2002–2017, and the data have been used to estimate changes in ice mass for glaciated areas around the world (Gardner, et al. 2013). The GRACE footprint is very large; in a region the size of Svalbard, mass change is computed for a handful of pixels. Furthermore, corrections must be made for ongoing and long-term isostatic rebound. However, satellite gravimetry also sidesteps problems with the other methods, such as the need to account separately for temporally varying calving or frontal retreat terms, or to extrapolate point measurements to larger areas. Nevertheless, a number of groups (Wouters, et al. 2008; Jacob, et al. 2012; Mémin, et al. 2011; Matsuo and Heki 2013; Gardner, et al. 2013) working with the same dataset covering slightly different periods, but using different data filtering methods, obtain a range of values for the total mass loss. The main conclusion one can reach from this body of work is that all find a negative mass balance from the Svalbard archipelago as whole, with values ranging from −0.46 to −0.09 m w.eq./yr, or −15.6 to −3.1 Gt/yr.

8. References

Aas, K., T. Dunse, E. Collier, T. V. Schuler, T. Berntsen, J. Kohler, and B. Luks, 2016. The climatic mass balance of Svalbard glaciers: a 10-year simulation with a coupled atmosphere–glacier mass balance model. *The Cryosphere*, 1089–1104.

AMAP, 2012. Arctic Climate Issues 2011: Changes in Arctic Snow, Water, Ice and Permafrost. SWIPA 2011 Overview Report. Arctic Monitoring and Assessment Programme (AMAP), Oslo, Norway.

AMAP, 2017. Snow, Water, Ice and Permafrost. Summary for Policy-makers. Arctic Monitoring and Assessment Programme (AMAP), Oslo, Norway.

Benestad, R. E., K. M. Parding, K. Isaksen, and A. Mezghani, 2016. Climate change and projections for the Barents region: what is expected to change and what will stay the same? *Environmental Research Letters* **11**(5), 054017, doi:10.1088/1748-9326/11/5/054017.

Bintanja, R. and F. M. Selten, 2014. Future increases in Arctic precipitation linked to local evaporation and sea-ice retreat. *Nature* **509**(7501), 479-482, doi:10.1038/nature13259.

Błaszczyk, M., J. A. Jania, and J. O. Hagen, 2009. Tidewater glaciers of Svalbard: Recent changes and estimates of calving fluxes. *Polish Polar Research* **30**(2), 85-142, doi:2007905507.

Brown, R., D. Vikhamar Schuler, O. Bulygina, C. Derksen, K. Luojus, L. Mudryk, L. Wang, and D. Yang, 2017. Arctic terrestrial snow cover. Pp. 25-64 in *Snow, Water, Ice and Permafrost in the Arctic (SWIPA) 2017*. Oslo, Norway: Arctic Monitoring and Assessment Programme (AMAP).

Christiansen, H. H., B. Etzelmüller, K. Isaksen, H. Juliussen, H. Farbrot, O. Humlum, M. Johansson, T. Ingeman-Nielsen, L. Kristensen, J. Hjort, P. Holmlund, A. B. K. Sannel, C. Sigsgaard, H. J. Åkerman, N. Foged, L. H. Blikra, M. A. Pernosky, and R. S. Ødegård, 2010. The thermal state of permafrost in the nordic area during the international polar year 2007-2009. *Permafrost and Periglacial Processes* **21**(2), 156-181, doi:10.1002/ppp.687.

Collins, M., R. Knutti, J. Arblaster, J.-L. Dufresne, T. Fichefet, P. Friedlingstein, X. Gao, W. J. Gutowski, T. Johns, G. Krinner, M. Shongwe, C. Tebaldi, A. J. Weaver, and M. Wehner, 2013. Long-term Climate Change: Projections, Commitments and Irreversibility. in *Climate Change 2013: The Physical Science Basis. Contribution of Working Group I to the Fifth Assessment Report of the Intergovernmental Panel on Climate Change*. Cambridge, United Kingdom and New York, NY, USA: Cambridge University Press.

Day, J. J., J. L. Bamber, P. J. Valdes, and J. Kohler, 2012. The impact of a seasonally ice free Arctic Ocean on the temperature, precipitation and surface mass balance of Svalbard. *The Cryosphere* **6**(1), 35-50, doi:10.5194/tc-6-35-2012.

Etzelmüller, B., T. V. Schuler, K. Isaksen, H. H. Christiansen, H. Farbrot, and R. Benestad, 2011. Modeling the temperature evolution of Svalbard permafrost during the 20th and 21st century. *The Cryosphere* **5**(1), 67-79, doi:10.5194/tc-5-67-2011.

Førland, E. J., R. Benestad, I. Hanssen-Bauer, J. E. Haugen, and T. E. Skaugen, 2011. Temperature and Precipitation Development at Svalbard 1900–2100. *Advances in Meteorology* **2011**, 1-14, doi:10.1155/2011/893790.

Førland, E. J. and I. Hanssen-Bauer, 2000. Increased Precipitation in the Norwegian Arctic: True or False? *Climatic Change* **46**(4), 485-509, doi:10.1023/A:1005613304674.

Førland, E. J. and I. Hanssen-Bauer, 2003. Past and future climate variations in the Norwegian Arctic: overview and novel analyses. *Polar Research* **22**(2), 113-124, doi:10.1111/j.1751-8369.2003.tb00102.x.

Forsström, S., E. Isaksson, R. B. Skeie, J. Ström, C. A. Pedersen, S. R. Hudson, T. K. Berntsen, H. Lihavainen, F. Godtliebsen, and S. Gerland, 2013. Elemental carbon measurements in European Arctic snow packs. *Journal of Geophysical Research Atmospheres* **118**(24), 13614-13627, doi:10.1002/2013JD019886.

Gardner, A. S., G. Moholdt, J. G. Cogley, B. Wouters, A. A. Arendt, J. Wahr, E. Berthier, R. Hock, W. T. Pfeffer, G. Kaser, S. R. M. Ligtenberg, T. Bolch, M. J. Sharp, J. O. Hagen, M. R. van den Broeke, and F. Paul, 2013. A reconciled estimate of glacier contributions to sea level rise: 2003 to 2009. *Science* **340**(6134), 852-7, doi:10.1126/science.1234532.

Gjelten, H. M., Ø. Nordli, K. Isaksen, E. J. Førland, P. N. Sviashchennikov, P. Wyszynski, U. V. Prokhorova, R. Przybylak, B. V. Ivanov, and A. V. Urazgildeeva, 2016. Air temperature variations and gradients along the coast and fjords of western Spitsbergen. *Polar Research* **35**(1), 29878, doi:10.3402/polar.v35.29878.

Gogoi, M. M., S. S. Babu, K. K. Moorthy, R. C. Thakur, J. P. Chaubey, and V. S. Nair, 2016. Aerosol black carbon over Svalbard regions of Arctic. *Polar Science* **10**(1), 60-70, doi:10.1016/j.polar.2015.11.001.

Graham, R. M., L. Cohen, A. A. Petty, L. N. Boisvert, A. Rinke, S. R. Hudson, M. Nicolaus, and M. A. Granskog, 2017a. Increasing frequency and duration of Arctic winter warming events. *Geophysical Research Letters* **44**(13), 6974-6983, doi:10.1002/2017GL073395.

Graham, R. M., A. Rinke, L. Cohen, S. R. Hudson, V. P. Walden, M. A. Granskog, W. Dorn, M. Kayser, and M. Maturilli, 2017b. A comparison of the two Arctic atmospheric winter states observed during N-ICE2015 and SHEBA. *Journal of Geophysical Research: Atmospheres* **122**(11), 5716-5737, doi:10.1002/2016JD025475.

Grenfell, T. C. and D. K. Perovich, 2008. Incident spectral irradiance in the Arctic Basin during the summer and fall. *Journal of Geophysical Research Atmospheres* **113**(12), 1-13, doi:10.1029/2007JD009418.

Hagen, J. O., J. Kohler, K. Melvold, and J.-G. Winther, 2003. Glaciers in Svalbard: mass balance, runoff and freshwater flux. *Polar Research* **22**(2), 145-159, doi:10.1111/j.1751-8369.2003.tb00104.x.

Hagen, J. O. and O. Liestøl, 1990. Long-Term Glacier Mass-Balance Investigations in Svalbard, 1950–88. *Annals of Glaciology* **14**, 102-106, doi:10.3189/S0260305500008351.

Hansen, J. R., 2010. Status og utviklingstrekk for klimaindikatorer i norsk del av Arktis MOSJ-rapport – klima. The Norwegian Polar Institute.

Hansen, B. B., K. Isaksen, R. E. Benestad, J. Kohler, Å. Ø. Pedersen, L. E. Loe, S. J. Coulson, J. O. Larsen, and Ø. Varpe, 2014. Warmer and wetter winters: characteristics and implications of an extreme weather event in the High Arctic. *Environmental Research Letters* **9**(11), 114021, doi:10.1088/1748-9326/9/11/114021.

Hanssen-Bauer, I. and E. J. Førland, 1998. Long-term trends in precipitation and temperature in the Norwegian Arctic: can they be explained by changes in atmospheric circulation patterns? *Climate Research* **10**(2), 143-153, doi:10.2307/24865962.

Hartmann, D. L., A. M. G. Klein Tank, M. Rusticucci, L. V. Alexander, S. Brönnimann, Y. Charabi, F. J. Dentener, E. J. Dlugokencky, D. R. Easterling, A. Kaplan, B. J. Soden, P. W. Thorne, M. Wild, and P. M. Zha, 2013. Observations: Atmosphere and Surface. Pp. 159-254 in *Climate Change 2013: The Physical Science Basis. Contribution of Working Group I to the Fifth Assessment Report of the Intergovernmental Panel on Climate Chan*, edited by T.F. Stocker, D. Qin, G.-K. Plattner, M. Tignor, S.K. Allen, J. Boschung, A. Nauels, Y. Xia, V. Bex, and P.M. Midgley. Cambridge, United Kingdom and New York, NY, US: Cambridge University Press.

Instanes, A. and J. L. Rongved, 2017. Forventede klimaendringers påvirkning på byggegrunn i Longyearbyen - området Delrapport 2 i oppdraget «Bygging og forvaltning på Svalbard i et langsiktig Klimaperspektiv». Statsbygg.

IPCC, 2013. Summary for Policymakers. in *Climate Change 2013: The Physical Science Basis. Contribution of Working Group I to the Fifth Assessment Report of the Intergovernmental Panel on Climate Change*, edited by T. F. Stocker, D. Qin, G.-K. Plattner, M. Tignor, S. K. Allen, J. Boschung, A. Nauels, Y. Xia, V. Bex, and P. M. Midgley. Cambridge, United Kingdom and New York, NY, USA: Cambridge University Press.

Irannezhad, M., A.-K. Ronkanen, and B. Kløve, 2016. Wintertime climate factors controlling snow resource decline in Finland. *International Journal of Climatology* **36**(1), 110-131, doi:10.1002/joc.4332.

Isaksen, K., E. J. Førland, A. Dobler, R. Benestad, J. E. Haugen, and A. Mezghani, 2017. Klimascenarioer for Longyearbyen-området , Svalbard. Delrapport 1, Statsbygg oppdrag: «Bygging og forvaltning på Svalbard i et langsiktig klimaperspektiv». METreport 15/2017.

Isaksen, K., Ø. Nordli, E. J. Førland, E. Łupikasza, S. Eastwood, and T. Niedźwiedź, 2016. Recent warming on Spitsbergen-Influence of atmospheric circulation and sea ice cover. *Journal of Geophysical Research: Atmospheres* **121**(20), 11,913-11,931, doi:10.1002/2016JD025606.

Isaksen, K., J. L. Sollid, P. Holmlund, and C. Harris, 2007. Recent warming of mountain permafrost in Svalbard and Scandinavia. *Journal of Geophysical Research* **112**(F2), F02S04, doi:10.1029/2006JF000522.

Jacob, T., J. Wahr, W. T. Pfeffer, and S. Swenson, 2012. Recent contributions of glaciers and ice caps to sea level rise. *Nature* **482**(7386), 514-518, doi:10.1038/nature10847.

James, T., T. Murray, N. E. Barrand, H. J. Sykes, A. J. Fox, and K. M.A., 2012. Observations of enhanced thinning in the upper reaches of Svalbard glaciers. *The Cryosphere*, 1369–1381.

Jorgenson, M. T., Y. L. Shur, and E. R. Pullman, 2006. Abrupt increase in permafrost degradation in Arctic Alaska. *Geophysical Research Letters* **33**(2), L02503, doi:10.1029/2005GL024960.

Kaser, G., J. G. Cogley, M. B. Dyurgerov, M. F. Meier, and A. Ohmura, 2006. Mass balance of glaciers and ice caps: Consensus estimates for 1961–2004. *Geophysical Research Letters* **33**(19), L19501, doi:10.1029/2006GL027511.

Koenigk, T., P. Berg, and R. Döscher, 2015. Arctic climate change in an ensemble of regional CORDEX simulations. *Polar Research* **34**(1), 24603, doi:10.3402/polar.v34.24603.

Kohler, J., T. D. James, T. Murray, C. Nuth, O. Brandt, N. E. Barrand, H. F. Aas, and A. Luckman, 2007. Acceleration in thinning rate on western Svalbard glaciers. *Geophysical Research Letters* **34**(18), L18502, doi:10.1029/2007GL030681.

König, M., C. Nuth, J. Kohler, G. Moholdt, and R. Pettersen, 2014. A digital glacier database for Svalbard. in *Global Land Ice Measurements from Space*, edited by J.S. Kargel, G.J. Leonard, M.P. Bishop, A. Kääb, and B.H. Raup. Springer-Verlag Berlin Heidelberg.

Kononova, N. K., 2012. The Influence of atmospheric circulation on the formation of snow cover on the north eastern Siberia. *Ice and Snow* **52**(1), 38-53, doi:10.15356/2076-6734-2012-1-38-53.

Koven, C. D., E. A. G. Schuur, C. Schädel, T. J. Bohn, E. J. Burke, G. Chen, X. Chen, P. Ciais, G. Grosse, J. W. Harden, D. J. Hayes, G. Hugelius, E. E. Jafarov, G. Krinner, P. Kuhry, D. M. Lawrence, A. H. MacDougall, S. S. Marchenko, A. D. McGuire, S. M. Natali, D. J. Nicolsky, D. Olefeldt, S. Peng, V. E. Romanovsky, K. M. Schaefer, J. Strauss, C. C. Treat, and M. Turetsky, 2015. A simplified, data-constrained approach to estimate the permafrost carbon-climate feedback. *Philosophical transactions. Series A, Mathematical, physical, and engineering sciences* **373**(2054), 20140423, doi:10.1098/rsta.2014.0423.

Lang, C., X. Fettweis, and M. Erpicum, 2015. Future climate and surface mass balance of Svalbard glaciers in an RCP8.5 climate scenario: a study with the regional climate model MAR forced by MIROC5. *The Cryosphere* **9**(3), 945-956, doi:10.5194/tc-9-945-2015.

Liljedahl, A. K., J. Boike, R. P. Daanen, A. N. Fedorov, G. V. Frost, G. Grosse, L. D. Hinzman, Y. Iijma, J. C. Jorgenson, N. Matveyeva, M. Necsoiu, M. K. Raynolds, V. E. Romanovsky, J. Schulla, K. D. Tape, D. A. Walker, C. J. Wilson, H. Yabuki, and D. Zona, 2016. Pan-Arctic ice-wedge degradation in warming permafrost and its influence on tundra hydrology. *Nature Geoscience* **9**(4), 312-318, doi:10.1038/ngeo2674.

Luckman, A., D. I. Benn, F. Cottier, S. L. Bevan, F. Nilsen, and M. E. Inall, 2015. Calving rates at tidewater glaciers vary strongly with ocean. *Nature Communications,* 8566–8572.

Matsuo, K. and K. Heki, 2013. Current Ice Loss in Small Glacier Systems of the Arctic Islands (Iceland, Svalbard, and the Russian High Arctic) from Satellite Gravimetry. *Terrestrial, Atmospheric and Oceanic Sciences* **24**(4-1), 657, doi:10.3319/TAO.2013.02.22.01(TibXS).

Maturilli, M., A. Herber, and G. König-Langlo, 2015. Surface Radiation Climatology for Ny-Ålesund, Svalbard (78.9° N), Basic Observations for Trend Detection. *Theoretical and Applied Climatology* **120**(1–2), 331-339, doi:10.1007/s00704-014-1173-4.

Meehl, G. A., C. Covey, T. Delworth, M. Latif, B. McAvaney, J. F. B. Mitchell, R. J. Stouffer, K. E. Taylor, G. A. Meehl, C. Covey, T. Delworth, M. Latif, B. McAvaney, J. F. B. Mitchell, R. J. Stouffer, and K. E. Taylor, 2007. THE WCRP CMIP3 Multimodel Dataset: A New Era in Climate Change Research. *Bulletin of the American Meteorological Society* **88**(9), 1383-1394, doi:10.1175/BAMS-88-9-1383.

Mémin, A., Y. Rogister, J. Hinderer, O. C. Omang, and B. Luck, 2011. Secular gravity variation at Svalbard (Norway) from ground observations and GRACE satellite data. *Geophysical Journal International* **184**(3), 1119-1130, doi:10.1111/j.1365-246X.2010.04922.x.

Moholdt, G., C. Nuth, J. O. Hagen, and J. Kohler, 2010. Recent elevation changes of Svalbard glaciers derived from ICESat laser altimetry. *Remote Sensing of Environment* **114**(11), 2756-2767, doi:10.1016/J.RSE.2010.06.008.

Möller, M., F. Obleitner, C. H. Reijmer, V. A. Pohjola, P. Głowacki, and J. Kohler, 2016. Adjustment of regional climate model output for modeling the climatic mass balance of all glaciers on Svalbard. *Journal of Geophysical Research: Atmospheres* **121**(10), 5411-5429, doi:10.1002/2015JD024380.

Myhre, C. L., O. Hermansen, M. Fiebig, C. R. Lunder, A. M. Fjæraa, K. Stebel, S. M. Platt, T. M. Svendby, J. N. Schmidbauer, and T. Krognes, 2015. Monitoring of greenhouse gases and aerosols at Svalbard and Birkenes in 2014 – Annual report. NILU, Kjeller.

Myhre, C. L., T. Svendby, O. Hermansen, C. Lunder, M. Fiebig, A. M. Fjæraa, G. Hansen, N. Schmidbauer, and T. Krognes, 2017. Monitoring of greenhouse gases and aerosols at Svalbard and Birkenes in 2016 – Annual report. NILU, Kjeller.

Nuth, C., J. Kohler, M. König, A. von Deschwanden, J. O. M. G. Hagen, and R. Pettersson, 2013. Decadal changes from a multi-temporal glacier inventory of Svalbard. *The Cryosphere*, 1603–1621.

Nuth, C., G. Moholdt, J. Kohler, J. O. Hagen, and A. Kääb, 2010. Svalbard glacier elevation changes and contribution to sea level rise. *Journal of Geophysical Research* **115**(F1), F01008, doi:10.1029/2008JF001223.

Onarheim, I. H., L. H. Smedsrud, R. B. Ingvaldsen, and F. Nilsen, 2014. Loss of sea ice during winter north of Svalbard. *Tellus A: Dynamic Meteorology and Oceanography* **66**(1), 23933, doi:10.3402/tellusa.v66.23933.

Overland, J., E. Hanna, I. Hanssen-Bauer, S. J. Kim, J. E. Walsh, M. Wang, U. S. Bhatt, and R. L. Thomam, 2015. "Surface Air Temperature [in Arctic Report Card 2015]." Arctic Report Card 2015. (http://www.arctic.noaa.gov/reportcard).

Overland, J., J. Walsh, and V. Kattsov, 2017. Trends and Feedbacks. Pp. 9-23 in *Snow, Water, Ice and Permafrost in the Arctic (SWIPA) 2017*. Oslo, Norway: Arctic Monitoring and Assessment Programme (AMAP).

Rasmus, S., J. Boelhouwers, A. Briede, I. A. Brown, M. Falarz, S. Ingvander, J. Jaagus, L. Kitaev, A. Mercer, and E. Rimkus, 2015. Recent Change—Terrestrial Cryosphere. Pp. 117-129 in *Second Assessment of Climate Change for the Baltic Sea Basin*, edited by The BACC II Author Team. Springer, Cham.

Raynolds, M. K., D. A. Walker, K. J. Ambrosius, J. Brown, K. R. Everett, M. Kanevskiy, G. P. Kofinas, V. E. Romanovsky, Y. Shur, and P. J. Webber, 2014. Cumulative geoecological effects of 62 years of infrastructure and climate change in ice-rich permafrost landscapes, Prudhoe Bay Oilfield, Alaska. *Global Change Biology* **20**(4), 1211-1224, doi:10.1111/gcb.12500.

Romanovsky, V., K. Isaksen, D. Drozdov, O. Anisimov, A. Instanes, M. Leibman, A. D. Mcguire, N. Shiklomanov, S. Smith, and D. Walker, 2017. Changing permafrost and its impacts. Pp. 65-102 in *Snow, Water, Ice and Permafrost in the Arctic (SWIPA) 2017*. Oslo, Norway: Arctic Monitoring and Assessment Programme (AMAP).

Romanovsky, V. E., S. L. Smith, and H. H. Christiansen, 2010. Permafrost thermal state in the polar Northern Hemisphere during the international polar year 2007-2009: a synthesis. *Permafrost and Periglacial Processes* **21**(2), 106-116, doi:10.1002/ppp.689.

Ruppel, M. M., I. Isaksson, J. Ström, E. Beaudon, J. Svensson, C. A. Pedersen, and A. Korhola, 2014. Increase in elemental carbon values between 1970 and 2004 observed in a 300-year ice core from Holtedahlfonna (Svalbard). *Atmospheric Chemistry and Physics* **14**(20), 11447-11460, doi:10.5194/acp-14-11447-2014.

Ruppel, M. M., J. Soares, J. C. Gallet, E. Isaksson, T. Martma, J. Svensson, J. Kohler, C. A. Pedersen, S. Manninen, A. Korhola, and J. Ström, 2017. Do contemporary (1980-2015) emissions determine the elemental carbon deposition trend at Holtedahlfonna glacier, Svalbard? *Atmospheric Chemistry and Physics* **17**(20), 12779-12795, doi:10.5194/acp-17-12779-2017.

Schuur, E. A. G., J. Bockheim, J. G. Canadell, E. Euskirchen, C. B. Field, S. V. Goryachkin, S. Hagemann, P. Kuhry, P. M. Lafleur, H. Lee, G. Mazhitova, F. E. Nelson, A. Rinke, V. E. Romanovsky, N. Shiklomanov, C. Tarnocai, S. Venevsky, J. G. Vogel, and S. A. Zimov, 2008. Vulnerability of Permafrost Carbon to Climate Change: Implications for the Global Carbon Cycle. *BioScience* **58**(8), 701-714, doi:10.1641/B580807.

Schuur, E. A. G., A. D. McGuire, C. Schädel, G. Grosse, J. W. Harden, D. J. Hayes, G. Hugelius, C. D. Koven, P. Kuhry, D. M. Lawrence, S. M. Natali, D. Olefeldt, V. E. Romanovsky, K. Schaefer, M. R. Turetsky, C. C. Treat, and J. E. Vonk, 2015. Climate change and the permafrost carbon feedback. *Nature* **520**(7546), 171-179, doi:10.1038/nature14338.

Sinha, P. R., Y. Kondo, K. Goto-Azuma, Y. Tsukagawa, K. Fukuda, M. Koike, S. Ohata, N. Moteki, T. Mori, N. Oshima, E. J. Førland, M. Irwin, J. C. Gallet, and C. A. Pedersen, 2018. Seasonal Progression of the Deposition of Black Carbon by Snowfall at Ny-Ålesund, Spitsbergen. *Journal of Geophysical Research: Atmospheres* **123**(2), 997-1016, doi:10.1002/2017JD028027.

Smith, S. L., V. E. Romanovsky, A. G. Lewkowicz, C. R. Burn, M. Allard, G. D. Clow, K. Yoshikawa, and J. Throop, 2010. Thermal state of permafrost in North America: a contribution to the international polar year. *Permafrost and Periglacial Processes* **21**(2), 117-135, doi:10.1002/ppp.690.

Spielhagen, R. F., K. Werner, S. A. Sørensen, K. Zamelczyk, E. Kandiano, G. Budeus, K. Husum, T. M. Marchitto, and M. Hald, 2011. Enhanced modern heat transfer to the Arctic by warm Atlantic Water. *Science (New York, N.Y.)* **331**(6016), 450-3, doi:10.1126/science.1197397.

Strand, S. M., 2016. Ground temperature response to winter warm events in Svalbard. Master thesis, Department of Geosciences, University of Oslo.

Svendby, T. M., G. H. Hansen, K. Stebel, A. Bäcklund, and A. Dahlback, 2017. Monitoring of the atmospheric ozone layer and natural ultraviolet radiation. Annual report 2016. NILU, Kjeller.

van Pelt, W. J. J., J. Kohler, G. E. Liston, J. O. Hagen, B. Luks, C. H. Reijmer, and V. A. Pohjola, 2016. Multidecadal climate and seasonal snow conditions in Svalbard. *Journal of Geophysical Research: Earth Surface* **121**(11), 2100-2117, doi:10.1002/2016JF003999.

van Pelt, W. J. J., J. Oerlemans, C. H. Reijmer, V. A. Pohjola, R. Pettersson, and J. H. van Angelen, 2012. Simulating melt, runoff and refreezing on Nordenskiöldbreen, Svalbard, using a coupled snow and energy balance model. *The Cryosphere* **6**(3), 641-659, doi:10.5194/tc-6-641-2012.

Vihma, T., J. Screen, M. Tjernström, B. Newton, X. Zhang, V. Popova, C. Deser, M. Holland, and T. Prowse, 2016. The atmospheric role in the Arctic water cycle: A review on processes, past and future changes, and their impacts. *Journal of Geophysical Research: Biogeosciences* **121**(3), 586-620, doi:10.1002/2015JG003132.

Vikhamar-Schuler, D., K. Isaksen, J. E. Haugen, H. Tømmervik, B. Luks, T. V. Schuler, J. W. Bjerke, D. Vikhamar-Schuler, K. Isaksen, J. E. Haugen, H. Tømmervik, B. Luks, T. V. Schuler, and J. W. Bjerke, 2016. Changes in Winter Warming Events in the Nordic Arctic Region. *Journal of Climate* **29**(17), 6223-6244, doi:10.1175/JCLI-D-15-0763.1.

Vincent, L. A., X. Zhang, R. D. Brown, Y. Feng, E. Mekis, E. J. Milewska, H. Wan, X. L. Wang, L. A. Vincent, X. Zhang, R. D. Brown, Y. Feng, E. Mekis, E. J. Milewska, H. Wan, and X. L. Wang, 2015. Observed Trends in Canada's Climate and Influence of Low-Frequency Variability Modes. *Journal of Climate* **28**(11), 4545-4560, doi:10.1175/JCLI-D-14-00697.1.

WMO, 2017. Greenhouse Gas Bulletin. The State of Greenhouse Gases in the Atmosphere Based on Global Observations through 2016. Geneva.

Wood, K. R. and J. E. Overland, 2010. Early 20th century Arctic warming in retrospect. *International Journal of Climatology* **30**(9), 1269-1279, doi:10.1002/joc.1973.

Wouters, B., D. Chambers, and E. J. O. Schrama, 2008. GRACE observes small-scale mass loss in Greenland. *Geophysical Research Letters* **35**(20), L20501, doi:10.1029/2008GL034816.

Zhang, T., R. G. Barry, K. Knowles, F. Ling, and R. L. Armstrong, 2003. Distribution of seasonally and perennially frozen ground in the Northern Hemisphere. Pp. 1289-1294 in *Permafrost*, edited by Springman & Arenson. Lisse: Swets & Zeitlinger.

Ørbæk, J. B., V. Hisdal, and L. E. Svaasand, 1999. Radiation climate variability in Svalbard: surface and satellite observations. *Polar Research* **18**(2), 127-134, doi:10.3402/polar.v18i2.6565.

Østby, T. I., T. V. Schuler, J. O. Hagen, R. Hock, J. Kohler, and C. H. Reijmer, 2017. Diagnosing the decline in climatic mass balance of glaciers in Svalbard over 1957-2014. *The Cryosphere* **11**(1), 191-215, doi:10.5194/tc-11-191-2017.

050 KORTRAPPORT / BRIEF REPORT
NORSK POLARINSTITUTT / NORWEGIAN POLAR INSTITUTE 2019